

Diatom shifts and limnological changes in a Siberian boreal lake: a multiproxy perspective on~~impacts of~~ climate warming and anthropogenic air pollution

5

Amelie Stieg^{1,2}, Boris K. Biskaborn¹, Ulrike Herzschuh^{1,2,3}, Andreas Marent¹, Jens Strauss¹, Dorothee Wilhelms-Dick⁴, Luidmila A. Pestryakova⁵, Hanno Meyer¹

¹Alfred Wegener Institute Helmholtz Centre for Polar and Marine Research, Potsdam, 14473, Germany.

10 ²Institute of Environmental Science and Geography, University of Potsdam, Potsdam, 14476, Germany.

³Institute of Biochemistry and Biology, University of Potsdam, Potsdam, 14476, Germany.

⁴Alfred Wegener Institute Helmholtz Centre for Polar and Marine Research, Bremerhaven, 27568, Germany.

⁵Institute of Natural Sciences, North-Eastern Federal University of Yakutsk, Yakutsk, 677007, Russia.

15

Correspondence to: Amelie Stieg (amelie.stieg@awi.de), Hanno Meyer (hanno.meyer@awi.de)

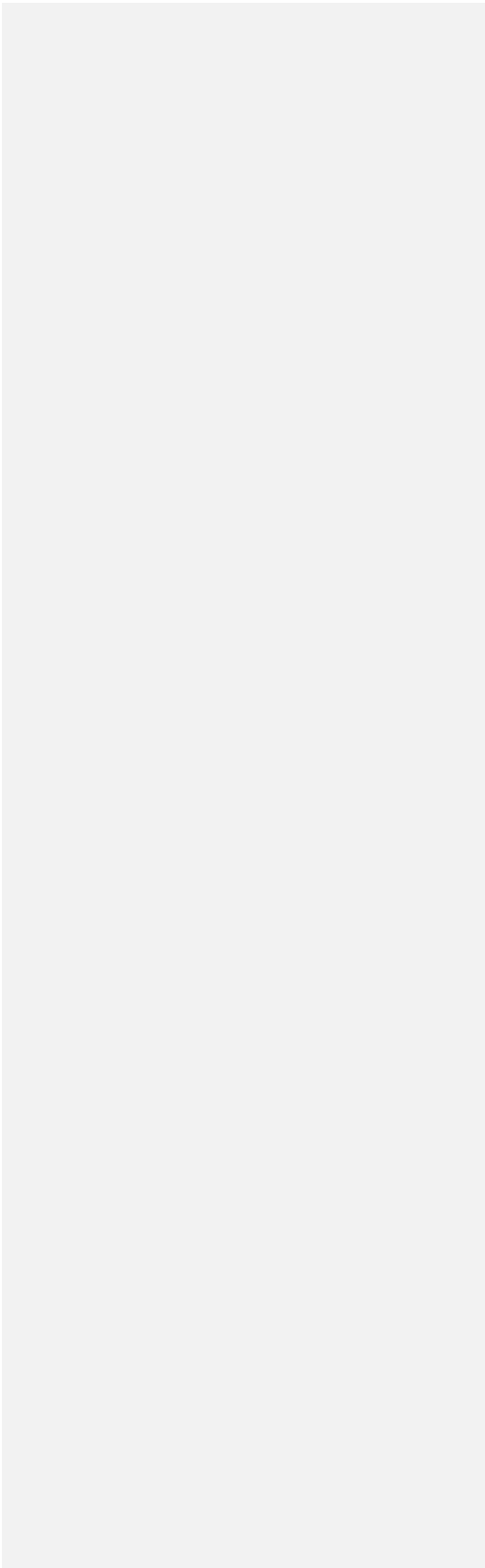
Formatiert: Schriftart: Kursiv

Abstract. Lake ecosystems are affected globally by climate warming and anthropogenic influences. However, impacts on boreal lake ecosystems in eastern Siberia, remain largely underexplored. Our aim is to determine if shifts in diatom assemblages in a remote lake in eastern Siberia are related to climate warming, similar to observations in temperate regions, while also exploring how the ecosystem might be influenced by hydroclimate and human-induced air pollution, through various biogeochemical proxies. We analysed continuous sediment samples from a ^{210}Pb – ^{137}Cs -dated short core from Lake Khamra (59.99° N, 112.98° E), covering ~220 years (ca. 1790–2015 CE), with the specific feature of following a multiproxy approach combining a variety of proxies on the same sample material to provide a comprehensive record of environmental changes in this less-examined/understudied region. Biogeochemical proxies include total organic carbon (TOC) and total nitrogen (TN) concentrations (TOC, TN) and corresponding stable isotopes of bulk sediment samples ($\delta^{13}\text{C}$, $\delta^{15}\text{N}$), as well as diatom silicon isotopes ($\delta^{30}\text{Si}_{\text{diatom}}$), alongside light microscope diatom species analysis. The diatom assemblage at Lake Khamra is dominated by few planktonic species, primarily *Aulacoseira subarctica* and *Aulacoseira ambigua*. At 1970 CE, we observe a significant major shift in diatom assemblages, characterised by with a marked increase in the planktonic species *Discostella stelligera* and a decrease in both *Aulacoseira* taxa. We, which we attribute these changes to recent global warming, which is likely associated with earlier ice-out, and potential enhanced summer thermal stratification, aligning consistent with similar observation changes seen in temperate lake ecosystems. In addition, we observe a rapid increase in chrysophyte scales (*Mallomonas*) since the 1990s further, supporting an increasing thermal stratification of the lake driven by rising temperatures. Biogeochemical proxies indicate substantial limnological changes around 1950 CE, preceding the major shift in diatom communities from 1970 CE onward. These earlier changes were, likely driven by hydroclimatic variability, and possibly influenced by fire-related disturbances in the catchment. Furthermore, we see evidence for an increased diatom productivity supported by rising diatom valve concentrations and accumulation rates. Sedimentary TOC and TN Carbon and nitrogen levels increase in the 1950s, preceding the 1970 CE shift in diatom assemblages, suggesting that rising precipitation after a dry period in the 1950s and hydroclimatic and fire-related changes in the catchment likely contributed to an increased allochthonous transport of organic material into the lake significantly influence the limnology. Increased precipitation and weathering are further discussed to alter in order to explain changing silica sources leading to decreasing $\delta^{30}\text{Si}_{\text{diatom}}$ after 1970 CE. Nevertheless, interpretation of $\delta^{30}\text{Si}_{\text{diatom}}$ in lacustrine systems is complex, likely influenced by both in-lake biogeochemical processes and catchment dynamics and suggest $\delta^{30}\text{Si}_{\text{diatom}}$ as a proxy for weathering rather than productivity at Lake Khamra. Indications of human impact/anthropogenic influences on the lake ecosystem Lake Khamra include a $\delta^{13}\text{C}^{13}\text{C}$ -depletion, likely linked to fossil fuel combustion and its emissions, coinciding with industrial growth in Asia and Russia since the 1950s. As identified in a previous study, mercury levels in the same sediment support a possible influence of long-distance air pollution. Despite, we find no evidence for atmospheric nitrogen deposition, and changes in diatom species composition, such as the increased abundance of planktonic *Asterionella formosa*. Furthermore, we observe a clear acidification trend since the 1990s, marked by a drastic major increase in *Mallomonas* scales since the 1990s, related to increased thermal stratification. Strong correlation to mercury accumulation rates, determined in a previous study, indicates a long-distance air pollution trend. We conclude that the Lake Khamra ecosystem of Lake Khamra is profoundly/severely affected by climate warming and shows indications of human impact/influences despite its remote location and human-induced pollution. This, emphasising the urgent need for comprehensive research to address and mitigate these impacts on remote lake ecosystems in order to secure natural water resources.

Formatiert: Schriftart: Nicht Kursiv

Formatiert: Schriftart: Nicht Kursiv

Formatiert: Tiefgestellt



1 Introduction

Human activities, particularly the burning of fossil fuels, have contributed significantly to the 'Great Acceleration' of Earth System changes especially since the 1950s (Steffen et al., 2015). Since then, the incidence of major ecological shifts in lake ecosystems globally has increased, driven by both climate change and anthropogenic impacts (Huang et al., 2022). These lake observations align with the proposed onset of the 'Anthropocene' (Crutzen and Stoermer, 2000), though it has not been formally recognised as a distinct geological epoch (ICS, 2024, last access 18. November 2024), a geological epoch beginning in the mid-20th century, introduced by Crutzen and Stoermer (2000) and further supported by Zalasiewicz et al. (2017).

Globally lake surface temperatures have risen in recent decades (O'Reilly et al., 2015; Hampton et al., 2018), having numerous consequences like changing thermal stratification properties, longer ice-free periods and changing lake ecosystems like shifting biological communities (Smol et al., 2005; Saros et al., 2012; Hampton et al., 2017; Woolway et al., 2020). Extensive research on lakes in North America and Europe (Smol et al., 2005; Smol and Douglas, 2007; Rühland et al., 2008; Kahlert et al., 2020) has shown that climate warming and human activities lead to significant ecological changes on remote high latitude ecosystems. A circumpolar study revealed major changes in the biological communities in remote Arctic lakes related to climate warming, starting as early as in the 1850s (Smol et al., 2005). Lake Baikal, a thoroughly studied system, has experienced documented ecosystem changes driven by recent warming, including increased water temperatures and shorter ice-cover periods (Todd and Mackay, 2003; Mackay et al., 2006; Hampton et al., 2008; Moore et al., 2009; Hampton et al., 2014; Izmet'seva et al., 2016). However, there is a notable gap remains in understanding how these global changes impacted boreal lakes in remote and less-studied regions of eastern Siberia, such as like the Republic of Sakha (Yakutia), Siberia.

Yakutia, located in eastern Siberia (Fig. 1a), has experienced rapid climate warming, with annual air temperature trends showing an increase of 0.3 to 0.6°C per decade since 1966 (Gorokhov and Fedorov, 2018). Most meteorological stations report the highest temperature increases in winter, along with a rise in overall precipitation rates over the last 50 years (Gorokhov and Fedorov, 2018). Furthermore, climate warming is associated with an increase in wildfire activity (AMAP, 2021), also observed in Yakutia, which is partly due to anthropogenic alterations to the ecosystems including traditional agro-industrial burning practices and the expansion of industrial areas (Kirillina et al., 2020).

There are evidences that recent warming and human-induced pollution have limnological effects in Siberia. For example, Lake Baikal, the deepest lake on Earth, showed a reduced lake ice cover duration and stronger thermal stratification since the 1950s (Roberts et al., 2018) and Evidence suggests that recent warming and human-induced pollution are impacting limnological conditions in Siberia. For instance, a remote lakes in eastern Siberia, without direct human influence in the catchment, displays signs of industrialisation's legacy, with mercury contamination in its sediments and a trend of lake acidification are also affected by the aftermath of industrialisation (Biskaborn et al., 2021b), as indicated by mercury contamination of the lake sediments and a lake acidification trend.

Diatoms, microscopic unicellular algae prevalent in nearly all aquatic environments, are effective indicators of various environmental disturbances such as climate change, acidification, and nutrient enrichment (Smol and Stoermer, 2010). They can even be linked to wildfire activity (Rühland et al., 2000). Their remains, called frustules, are composed of biogenic silica ($\text{SiO}_2 \cdot n\text{H}_2\text{O}$), which are highly-resistant and well-preserved in lake sediments.

Diatom valves are suitable for light microscopic identification up to the highest species level (Battarbee et al.,

2001), as well as for oxygen and silicon isotope measurements to reconstruct past climate and environmental conditions (Leng and Barker, 2006; Sutton et al., 2018; Frings et al., 2024). (Leng and Barker, 2006). Circum-Arctic studies reveal climate warming, resulting in a shortened duration of lake ice covers and an extended growing season, along with thermal stratification of lake water, is the primary cause of the observed shift in diatom assemblages (Sorvari et al., 2002; Rühland et al., 2003; Rühland and Smol, 2005; Smol et al., 2005; Rühland et al., 2008; Rühland et al., 2015). However, Siberian lakes are underrepresented in circumpolar studies on diatom assemblage changes (Smol et al., 2005; Rühland et al., 2008). In Siberia, studies analysing paleolimnological studies in eastern Siberia, including Yakutia, have utilised conditions through diatom assemblages, combined with alongside diatom isotope $\delta^{30}\text{Si}$, or biogeochemical proxies such as organic carbon and nitrogen, and mercury analyses, are available to investigate past environmental conditions. However, many of these studies predominantly cover periods within the Quaternary, primarily focusing on the Holocene, and investigate long-term trends (e.g. (e.g. Cherapanova et al., 2006; Biskaborn et al., 2012; Pestryakova et al., 2012; Biskaborn et al., 2016; Biskaborn et al., 2021c; Firsova et al., 2021; Kostrova et al., 2021; Mackay et al., 2022; Biskaborn et al., 2023). While there is a growing body of work on recent environmental change in eastern Siberia, high-resolution studies covering shorter time periods in Yakutia remain rare. Studies focussing on shorter time periods with a higher resolution are rare in Yakutia. Besides a one study in the remote boreal areas in Yakutia of Siberia (Biskaborn et al., 2021b), notable study sites are located further south at Lake Baikal (Roberts et al., 2018), on Kamchatka (Jones et al., 2015), further north-west towards Europe (Palagushkina et al., 2020), or in the northern Urals (Solovieva et al., 2008). However, these sites are influenced by different climatic and ecological conditions that can differ from those in Yakutia. Even where paleoecological studies of shorter time periods exist, they often focus on Arctic environments or region further south, such as North China. Hence, even if there are paleoecological studies that refer to shorter time periods, the lakes investigated are either not located in Siberia, lie in the Arctic region, or are very far south influenced by different climate regimes, as for example in North China (Yan et al., 2018).

In a previous study at the boreal Lake Khamra in southwest Yakutia, a diatom oxygen isotope record ($\delta^{18}\text{O}_{\text{diatom}}$) was established to reconstruct hydroclimatic anomalies and suggested increasing (winter) precipitation along with rising air temperatures since the 1970s (Stieg et al., 2024b). Beside In addition to oxygen isotopes, silicon isotopes of diatoms have been used as indicators of changing productivity and nutrient utilization. are used as paleoenvironmental proxy, for example in a lake sediment record from South China (Chen et al., 2012). Predominantly, $\delta^{30}\text{Si}_{\text{diatom}}$ serves as a proxy for primary production in marine environments (De La Rocha et al., 1998; Sutton et al., 2018). In lacustrine systems, however, $\delta^{30}\text{Si}_{\text{diatom}}$ interpretation is more complex due to the combined influence of catchment processes (e.g. weathering, vegetation, soil development) and in-lake biogeochemical dynamics (e.g. silica cycling and sedimentation) (Sutton et al., 2018; van Hardenbroek et al., 2018; Frings et al., 2024). Research at Lake Baikal has explored the preservation and reliability of $\delta^{30}\text{Si}_{\text{diatom}}$ for paleo-reconstructions, as well as its link to diatom productivity and sedimentary processes (Panizzo et al., 2016; 2017; 2018). Despite these studies, spatial and temporal coverage of $\delta^{30}\text{Si}_{\text{diatom}}$ research in eastern Siberia remains limited. Furthermore, However, studies that analyse both oxygen and silicon isotopes of diatoms from the same samples are rather rare, with One example from a lake in northern Siberia focusing on the time period since the Last Glacial Maximum (Swann et al., 2010).

In this study, we analyse subfossil diatom assemblages in Lake Khamra to determine whether any taxonomic changes are consistent with recent climate warming, as documented in many temperate lakes in throughout North

Formatiert: Tiefgestellt

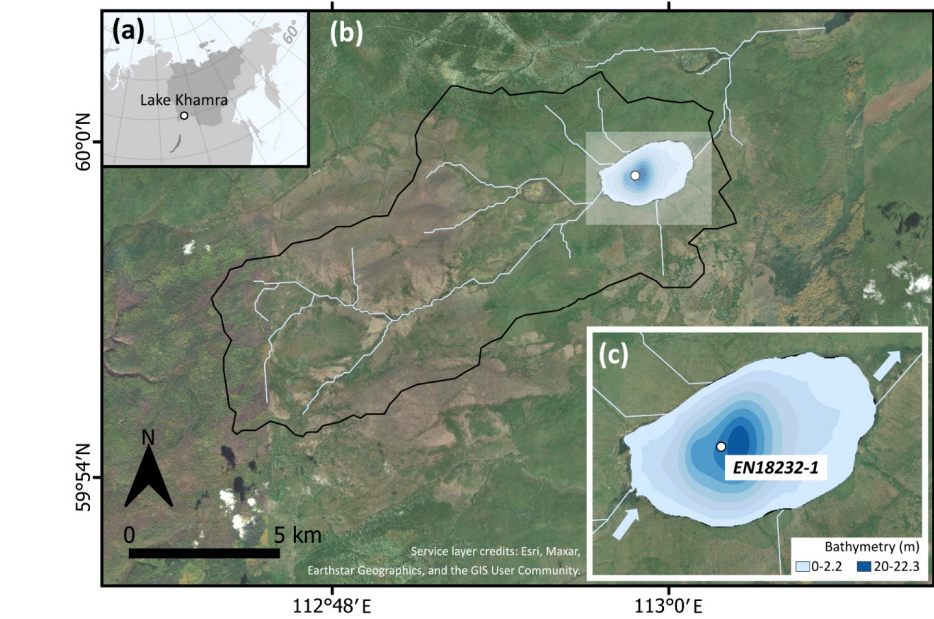
Formatiert: Tiefgestellt

Formatiert: Tiefgestellt

Formatiert: Tiefgestellt

~~America and Europe. Additionally, we test whether significant shifts in the Lake Khamra diatom assemblages occur, which can be related to climate warming, consistent with observations from temperate regions in North America and Europe. We also investigate potential limnological responses to climate and anthropogenic pollution impacts.~~ Our research addresses this ~~gap~~ by examining diatom assemblages and ~~various~~ biogeochemical proxies (TOC, TN, $\delta^{13}\text{C}$, $\delta^{15}\text{N}$, $\delta^{30}\text{Si}_{\text{diatom}}$) at decadal resolution since circa 1790 CE. ~~Using~~ We analyse continuous sediment samples from a short core of Lake Khamra, eastern Siberia, ~~we to~~ provide a detailed account of environmental changes. Our specific objectives are to (I) identify historical lake ecosystem changes within a continuous diatom assemblage record spanning the last ~220 years, (II) evaluate the origin of organic material and distinguish between allochthonous and autochthonous sources in response to hydroclimatic variations using biogeochemical proxies evaluate lake bioproductivity and erosional input linked to hydroclimatic variations through biogeochemical proxies, and (III) assess the impact of human-induced air pollution on diatom assemblages as well as the lake ecosystem.

2.1 Study site



160 Figure 1. (a) Location of Lake Khamra in eastern Siberia, with Yakutia highlighted in darker grey. (b) Catchment of Lake Khamra. (c) Bathymetry of Lake Khamra, main inflow in the SW, main outflow in the NE and coring location of drilling position of sediment core EN18232-1 in the central part of the lake. Service layer credits: Esri, Maxar, Earthstar Geographics, and the GIS User Community.

165 Lake Khamra (59.99° N, 112.98° E, 340 m a.s.l.) is located distant from direct human impact in the south-west of the Republic of Sakha (Yakutia), eastern Siberia, Russia, with the closest urban settlements, Peleduy and Vitim, situated 40 and 60 km to the south-west, respectively. The landscape is located in the transition zone of evergreen to deciduous needle leaf boreal forest within the ecoregion of the middle taiga (in (in Geng et al., 2022 after Stone and Schlesinger, 2004) after Stone and Schlesinger, 2004). According to field observations (Kruse et al., 2019; Miesner et al., 2022), the research area is covered by a mixed-coniferous forest. The annual mean ground temperature lies between 0.0–1.0 °C at a depth of 10–20 m (Shestakova et al., 2021), indicating that the study site is within a discontinuous to sporadic permafrost zone (Obu et al., 2019). Geologically, the region is underlain by 170 Cambrian bedrock composed of alternating dolomite and limestone, interspersed with silty Ordovician sandstone and patches of clayey Silurian limestone (Chelnokova et al., 1988).

The lake morphology is characterised by shallow shore areas and a nearly central deep part with a maximum water depth of 22.3 m (Fig. 1c). The lake has a surface area of 4.6 km² and a catchment size of 107.3 km². Lake Khamra 175 is a hydrologically open system with a main inflow in the south-west and an outflow in the north-east and an estimated average long-term discharge of 1.1 m³ s⁻¹ (Messenger et al., 2016). In winter, the lake is covered by ice and snow, observed with an average ice thickness of 0.5 m and an about 1 m thick snow cover in March 2020

(Biskaborn et al., 2021a). Temperatures measured in the water column during that time ranged from 2 to 2.7 °C. A surface water sample taken during a summer field campaign in 2018 revealed a pH value of 6.07 and a conductivity of 40 µS/cm (Stieg et al., 2024b).

The nearest weather station is located in the town of Vitim (59.45° N, 112.58° E; 186 m a.s.l.; ECA (European Climate Assessment) station code 3235). Details and a climate diagram for the study site can be found in Stieg et al. (2024b). In relation to this, the regional climate is continental, expressed in extremely cold and dry winters (January: -28.8°C mean temp., 1929–2018 CE) and warm and humid summers (July: +18.1°C mean temp., 1929–2018 CE). The annual precipitation average at Vitim reaches 423 mm (1929–2018 CE), while the mean annual air temperature is at -5.0 °C.

2.2 Fieldwork, subsampling and core dating

Coring activities at Lake Khamra were conducted during a summer expedition in 2018 (Kruse et al., 2019). The sediment short core EN18232-1 was obtained with an UWITEC Gravity corer (60 mm) from the central and deepest part of Lake Khamra (59.99091°N, 112.98373°E; 22.3 m), based on water–depth measurements determined with a surveying rope and a portable HONDEX PS-7 LCD digital sounder. The sediment core with a total length of 42 cm was sealed with water-absorbent floral foam and transported in a PVC tube to the Alfred Wegener Institute (AWI) in Potsdam, where it was stored dark and cool at 4°C until further analysis. The sediment core was subsampled downcore in horizontal 1-cm continuous increments (n=39) in October 2021. To avoid potential contamination between depths due to mixing, rim material (<0.5 cm) was carefully removed from each sample layer. The rim material (<0.5 cm) was removed to avoid possible contamination due to mixing. Furthermore, water content and dry bulk densities were determined (Stieg et al., 2024b). All subsamples were freeze-dried for at least 48 h before further processing.

We use the age–depth model for the short core EN18232-1 published by Stieg et al. (2024b), providing a comprehensive ~220-year record (ca. 2015–1790 CE, mean ages) with a sub-decadal resolution according to mean ages (5.7 ± 1.7 years). The chronology relies on analysis for ^{210}Pb , ^{226}Ra , ^{137}Cs , and ^{241}Am using direct gamma assay techniques with Ortec HPGe GWL series well-type coaxial low background intrinsic germanium detectors, conducted at the Liverpool University Environmental Radioactivity Laboratory as described by Appleby et al. (1986). The age–depth model of the short core was calculated with a Bayesian accumulation model within the R package ‘rbacon’ v2.5.8 (Blaauw and Christen, 2011; R version 4.1.1); ~~R version 4.1.1~~, based on the ^{210}Pb chronology, shown in Fig. A1 in the appendix. In addition, data on the water content and the average dry bulk density (DBD) of the short core were determined from selected subsamples (n=24) using a 1 cm³ tool taken at regular intervals, with weights measured before and after freeze-drying. The mean DBD (g cm⁻³) was then used together with the, with the latter being used to calculate sedimentation rates (SR, cm a⁻¹) and to calculate mass accumulation rates (MAR, g cm⁻² a⁻¹) downcore (full details given in Stieg et al., 2024a).

2.3.1.1 Biogeochemical proxies

~~The total organic carbon (TOC) and total nitrogen (TN) of 39 samples were determined to analyse historical changes of the organic matter content in the lake sediments. Freeze-dried subsamples were ground to obtain a homogeneous material. TOC was analysed by using an Elemental soil TOC cube. Total carbon (TC) was computed~~

Formatiert: Hochgestellt

by the sum of TOC and the total inorganic carbon (TIC), published in a previous study (Stieg et al., 2024b). Organic carbon accumulation rates (OCARs, $\text{g m}^{-2} \text{a}^{-1}$) were derived by dividing TOC by 100, multiplying it by the mass accumulation rates (MAR) $\times 10,000$ to $\text{g m}^{-2} \text{a}^{-1}$ unit. TN was quantified by an Elemental rapid-MAX N exceed. The measurement accuracy was 0.1 % for both devices, carried out at the BioGeoChemistry Lab at AWI Potsdam. The TOC/TN atomic ratio (C/N), as an indicator of the organic matter source, was calculated by multiplying its mass ratio by 1.167, which is the ratio of the atomic weights of nitrogen and carbon (Meyers and Teranes, 2001). The stable carbon isotope ratio ($^{13}\text{C}/^{12}\text{C}$) of all freeze-dried and milled samples was examined, to gain additional information on past productivity and organic matter sources. Prior to isotope measurement, inorganic carbon was removed by a hydrochloric acid treatment (HCl , 1.3 mol L^{-1}). Carbon isotopes were measured by a ThermoFisher Scientific Delta V Advantage gas mass spectrometer equipped with a FLASH elemental analyser EA 2000, a CONFLO IV gas mixing system and a MA200R autosampler at the ISOLAB of AWI Potsdam. Isotope ratios are given relative to laboratory standards of known isotopic compositions and relative to the Vienna Pee Dee Belemnite (VPDB) reference standard. Nitrogen isotope ratios ($^{15}\text{N}/^{14}\text{N}$) of the 39 samples were analysed using the same gas mass spectrometer and expressed relative to the standard atmospheric nitrogen ratio (air). Both isotope ratios are given as delta notation ($\delta^{13}\text{C}$, $\delta^{15}\text{N}$) in per mill (‰), with 1 σ standard errors better than ± 0.15 ‰.

2.4 — Diatom purification process and silicon isotopes

In a previous study (Stieg et al., 2024b), which focused on the oxygen isotopes of diatoms of the sediment short core EN18232-1, a comprehensive description of the diatom isotope purification procedure of the samples is provided. The silicon isotope composition was determined from the same aliquots (Leng and Sloane, 2008). In general, the purification assessment of diatom samples includes wet chemical as well as physical preparation steps (Morley et al., 2004; Leng and Barker, 2006). Essentially, the cleaning procedure included the removal of organic matter with H_2O_2 (30 %), eliminating carbonates by using HCl (10 %) and multiple heavy liquid separations (HLS) with sodium polytungstate solutions (SPT) with decreasing densities (EN18232-1: 2.50 – 2.12 g cm^{-3}) to separate the diatom valves from the heavy minerogenic fraction. High purity of the diatom samples was supported by a contamination assessment using a JEOL M-IT500HR analytical scanning electron microscope (SEM) with an integrated Energy Dispersive X-ray Spectroscopy (EDS) system.

The laser fluorination method was applied using bromine pentafluoride (BrF_3) as a reagent to completely extract oxygen from the diatom SiO_2 (Clayton and Mayeda, 1963), after employing the inert Gas Flow Dehydration method (Chapligin et al., 2010). The released silicon component combines thereby with BrF_3 to silicon tetrafluoride (SiF_4). The separation of SiF_4 from the bromine compounds was achieved using a cold trap, composed of a slush of ethanol-cooled with liquid nitrogen (N_2) at -115°C . SiF_4 was then transferred and trapped into Pyrex glass tubes for the subsequent silicon isotope analysis (Chapligin et al., 2010; Maier et al., 2013). For all samples ($n=39$) two SiF_4 extractions were performed (except two samples with only one extraction). The samples were measured 10 times on a MAT-252 IRMS at AWI Bremerhaven against a reference gas with known isotopic composition, calibrated to the reference quartz standard NBS-28. The data was processed for outliers by performing a Dixon test with a confidence level of 80 % (Dixon, 1953). The results are expressed as delta notation $\delta^{29}\text{Si}$ ($^{29}\text{Si}/^{28}\text{Si}$) in per mill (‰). The calibration was done with the internal biogenic silica standard BFC with a known $\delta^{29}\text{Si}$ of $+0.13$ ‰ relative to NBS-28 (Leng and Sloane, 2008). Analytical precision determined by repeated

analyses of the internal standard (n=12) was better than 0.07 ‰ (1σ of δ³⁰Si). A weighted mean value for each sample measurement was calculated with a standard deviation resulting from the internal or the external consistency, depending on which value is higher.

2.52.3 Diatom analysis

Diatom slides were prepared for each of the 39 samples of the short core EN18232-1 to analyse the species assemblages. Preparation of slides for siliceous microfossils followed common procedures. The slide preparation followed the common procedure Battarbee et al. (2001). Aliquots of 0.10 g freeze-dried sample material were treated with H₂O₂ (30 %) at 90°C for up to 8 h to remove organic matter. The reaction was stopped and carbonates were eliminated by adding HCl (10 %). After washing with purified water, 5-ml of Microsphere suspension (2 x 10⁶ microspheres ml⁻¹) were added to estimate the diatom valve concentration (DVC; (DVC, Battarbee and Kneen, 1982). In addition, 1 drop of ammonia (NH₃) solution was added to each sample to prevent clumping of diatom valves. The homogenised sample solution was transferred onto cover slips using Battarbee cups and mounted to slides using Naphrax. A minimum of 350 diatom valves in each sample were counted along transects (mean: 391 valves) by using a ZEISS AXIO Scope.A1 light microscope with a Plan-Apochromat 100x/ 1.4 Oil Ph3 objective at 1000x magnification. Diatom species were identified to lowest possible taxonomic level primarily by using classical identification literature (Krammer and Lange-Bertalot, 1991; Krammer et al., 1991; Krammer and Lange-Bertalot, 1997a, b; Hofmann et al., 2011), supported by regional (Russian) floras (Komarenko and Vasilyeva, 1975; Moiseeva and Nikolaev, 1992; Makarova, 2002). Diatom nomenclature and synonyms were applied using online databases such as Diatoms.org (<https://www.diatoms.org>; last access: 01. August 2024; (<https://www.diatoms.org>; last access: 01. August 2024; Spaulding et al., 2021) and AlgaeBase (<https://www.algaebase.org>; last access: 01. August 2024; (<https://www.algaebase.org>; last access: 01. August 2024; Guiry and Guiry, 2024), for some species further supported with input by members of the diatom community online platform DIATOM-L (Bahls, 2015).

In addition, silicified chrysophyte *Mallomonas* scales were counted without further specification to calculate the *Mallomonas* index, which measures *Mallomonas* in relation to diatom cells (M/D), to evaluate the degree of thermal stratification and the trophic status (Smol, 1985; Ginn et al., 2010), to evaluate lake acidification (Smol et al., 1984; Biskaborn et al., 2021b). The ratio of planktonic-to-benthic diatoms (P/B) of the most abundant species was calculated, excluding tychoplanktonic species, as an additional indicator of paleoenvironmental change. Habitat assignment followed mainly the online database Diatoms.org (<https://www.diatoms.org>; last access: 01. August 2024; (<https://www.diatoms.org>; last access: 01. August 2024; Spaulding et al., 2021) and habitat information from Barinova et al. (2011). Furthermore, the abundances of the dominant *Aulacoseira* species (*A. ulacoseira subarctica* and *A. ulacoseira ambigua*) were summarised to better identify the assemblage changes in relation to the planktonic taxa *Discostella stelligera*.

2.4 Diatom purification process and silicon isotopes

In a previous study (Stieg et al., 2024b), which focused on the oxygen isotopes of diatoms of the sediment short core EN18232-1, a comprehensive description of the diatom isotope purification procedure of the samples is provided. The silicon isotope composition was determined from the same aliquots (Leng and Sloane, 2008). In

general, the purification assessment of diatom samples includes wet chemical as well as physical preparation steps (Morley et al., 2004; Leng and Barker, 2006). Essentially, the cleaning procedure included the removal of organic matter with H_2O_2 (30 %), eliminating carbonates by using HCl (10 %) and multiple heavy liquid separations (HLS) with sodium polytungstate solutions (SPT) with decreasing densities (EN18232-1: 2.50–2.12 g cm⁻³) to separate the diatom valves from the heavy minerogenic fraction. High purity of the diatom samples was supported by a contamination assessment using a JEOL M-IT500HR analytical scanning electron microscope (SEM) with an integrated Energy-Dispersive X-ray Spectroscopy (EDS) system.

The laser fluorination method was applied using bromine pentafluoride (BrF_5) as a reagent to completely extract oxygen from the diatom SiO_2 (Clayton and Mayeda, 1963), after employing the inert Gas Flow Dehydration method (Chapligin et al., 2010). The released silicon component combines with BrF_5 to silicon tetrafluoride (SiF_4). The separation of SiF_4 from the bromine compounds was achieved using a cold trap, composed of a slush of ethanol cooled with liquid nitrogen (N_2) at -115 °C. SiF_4 was then transferred and trapped into Pyrex glass tubes for the subsequent silicon isotope analysis (Chapligin et al., 2010; Maier et al., 2013). For all samples (n=39) two SiF_4 extractions were performed (except two samples with only one extraction). The samples were measured 10 times on a MAT 252 IRMS at AWI Bremerhaven against a reference gas with known isotopic composition, calibrated to the reference quartz standard NBS-28. The data was processed for outliers by performing a Dixon test with a confidence level of 80 % (Dixon, 1953). The results are expressed as delta notation $\delta^{30}\text{Si}$ ($^{30}\text{Si} / ^{28}\text{Si}$) in per mill (‰). The calibration was done with the internal biogenic silica standard BFC with a known $\delta^{30}\text{Si}$ of +0.13 ‰ relative to NBS-28 (Leng and Sloane, 2008). Analytical precision determined by repeated analyses of the internal standard (n=12) was better than 0.07 ‰ (1 σ of $\delta^{30}\text{Si}$). A weighted mean value for each sample measurement was calculated with a standard deviation resulting from the internal or the external consistency, depending on which value is higher.

2.5 Biogeochemical proxies

The total organic carbon (TOC) and total nitrogen (TN) of 39 samples were determined to analyse historical changes of the organic matter content in the lake sediments. Freeze-dried subsamples were ground to obtain a homogeneous material. TOC was analysed by using an Elemental soli TOC cube. Total carbon (TC) was computed by the sum of TOC and the total inorganic carbon (TIC), published in a previous study (Stieg et al., 2024b). Organic carbon accumulation rates (OCARs, g m⁻² a⁻¹) were derived by dividing TOC by 100, multiplying it by the mass accumulation rates (MAR) * 10.000 to g m⁻² a⁻¹ unit. TN was quantified by an Elementar rapid MAX N exceed. The measurement accuracy was 0.1 % for both devices, carried out at the BioGeoChemistry Lab at AWI Potsdam. The TOC/TN atomic ratio (C/N), as an indicator of the organic matter source, was calculated by multiplying its mass ratio by 1.167, which is the ratio of the atomic weights of nitrogen and carbon (Meyers and Teranes, 2001). The stable carbon isotope ratio ($^{13}\text{C}/^{12}\text{C}$) of all freeze-dried and milled samples was examined, to gain additional information on past productivity and organic matter sources. Prior to isotope measurement, inorganic carbon was removed by a hydrochloric acid treatment (HCl , 1.3 mol L⁻¹). Carbon isotopes were measured by a ThermoFisher Scientific Delta-V-Advantage gas-mass spectrometer equipped with a FLASH elemental analyser EA 2000, a CONFLO IV gas-mixing system and a MA200R autosampler at the ISOLAB of AWI Potsdam. Isotope ratios are given relative to laboratory standards of known isotopic compositions and relative to the Vienna Pee Dee Belemnite (VPDB) reference standard. Nitrogen isotope ratios ($^{15}\text{N}/^{14}\text{N}$) of the 39 samples were analysed using

the same gas-mass spectrometer and expressed relative to the standard atmospheric nitrogen ratio (air). Both isotope ratios are given as delta notation ($\delta^{13}\text{C}$, $\delta^{15}\text{N}$) in per mill (‰), with 1 σ standard errors better than ± 0.15 ‰.

2.6 Data processing and statistical analyses

For data processing and statistical analyses, we used the R environment (R Core Team, 2024). Diatom species richness (alpha diversity) and evenness (effective richness) were assessed by calculating Hill's N0 and N2 (Hill, 1973), with a rarefaction of the data set based on the count's minimum ($n = 352$), to prevent biases of varying sample sizes, utilising the R package 'vegan' (Oksanen et al., 2022). By categorising the diatom counts into dissolved and pristine valves, the F index was calculated to assess the diatom valve dissolution (Ryves et al., 2001) after Flower and Likhoshway, 1993). The F index has a total range between 0 and 1, whereby 1 equals a perfect preservation.

For further processing, the total counts of diatom species were converted to percentage data. With the R package 'rioja' (Juggins, 2022) constrained incremental sums-of-squares clustering (CONISS) was performed to define diatom zones in the record, after square-root transformation and Euclidean dissimilarity calculation of the percentage data of all involved species using the 'vegan' package (Oksanen et al., 2022), to ensure all species contribute meaningfully to the analysis, regardless of their abundance (Grimm, 1987). The diatom relative abundances and CONISS clustering are presented in a stratigraphic diagram using the function 'strat.plot' of the 'rioja' package (Juggins, 2022). The stratigraphy plot displays the predominant species only, which occur at least twice (≥ 2 samples) with a minimum abundance of 2 %.

The length of gradient variation of the percentage data was determined by a detrended correspondence analysis (DCA), calculated in standard deviation units ($\text{SD} = 1.03$), using the 'decorana' function of the R package 'vegan' (Oksanen et al., 2022). Following the thresholds discussed in Birks (2010), a principal component analysis (PCA) was conducted on the most abundant species (≥ 2 % in ≥ 2 samples) after square-root transformation. Additionally, data of diatom isotopes and biogeochemical proxies of the same sediment samples ($\delta^{18}\text{O}_{\text{diatom}}$, $\delta^{30}\text{Si}_{\text{diatom}}$, TOC, TN, C/N, OCAR, $\delta^{13}\text{C}$, $\delta^{15}\text{N}$, mercury, diatom valve concentration, diatom accumulation rates DVC, DAR, M/D) were projected onto the PCA ordination plot of diatom data using the 'envfit' function (Oksanen et al., 2022), enabling the visualisation within the taxonomical and ecological context.

Diatom accumulation rates (DARs in 10^9 valves $\text{m}^{-2} \text{a}^{-1}$) were calculated by multiplying the diatom valve concentration (DVC in 10^7 valves g^{-1}) with mass accumulation rates (MAR, $\text{g cm}^{-2} \text{a}^{-1}$) according to Birks (2010) and multiplying it by 100 to convert it to 10^9 valves $\text{m}^{-2} \text{a}^{-1}$. Sediment proxies and diatom indices were correlated by performing a Pearson correlation by using the 'cor.test' function in the R package 'stats' (R Core Team, 2024) and displayed as correlation matrix with the package 'corrplot' (Wei and Simko, 2021).

Correlations with p -values < 0.05 were considered significant. In addition, data were correlated separately for periods before and after 1950 CE, employing mean ages, to specifically investigate possible anthropogenic effects in the lake ecosystem.

3 Results

3.11 Biogeochemical proxies and $\delta^{20}\text{Si}_{\text{diatom}}$

Formatiert: Überschrift 1

1 The TOC and TN records are strongly intercorrelated ($r = 0.98$, $p < 0.05$; Fig. 2, A2). TOC has a mean value of 9.2 % and TN has a mean of 0.9 %. Around 1800 CE, at the lower part of the core, both proxies are above their mean. Between ca. 1830–1940 CE, values decline and stay below their mean, including their minima at about 1875 CE (TOC = 7.5 %, TN = 0.7 %). At the onset of the 1950s, TOC and TN values rise above the mean again and increase nearly continuously since the 1970s, reaching both their total maxima in the uppermost sample (TOC = 12.5 %, TN = 1.2 %). The C/N ratio has a mean of 12.6 and varies by ± 1.4 . Until the 1950s, the C/N ratio fluctuates slightly between 12.5 and 13, including two maxima at around 1800 CE and 1895 CE. Around 1950 CE, the C/N ratio shifts to lower values of about 12. In the two uppermost samples, the ratio slightly increases again towards 12.5 (Fig. 2). The values of OCAR fluctuate slightly around the mean value of $20.5 \text{ g m}^{-2} \text{ a}^{-1}$ and only fall below it from the 1950s until a minimum of $11.5 \text{ g m}^{-2} \text{ a}^{-1}$ at around 1970 CE, before rising to the maximum value of $50.6 \text{ g m}^{-2} \text{ a}^{-1}$ in the youngest sample (Fig. 2).

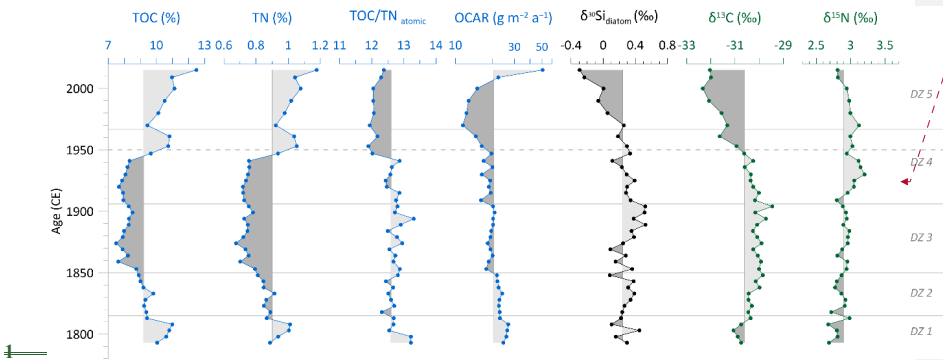
1 $\delta^{20}\text{Si}_{\text{diatom}}$ ranges between -0.29 to $+0.52$ ‰, with an overall mean of $+0.24$ ‰. Until 1970 CE, $\delta^{20}\text{Si}_{\text{diatom}}$ values stay mainly above the mean, including the absolute maximum of $+0.52$ ‰ around 1900 CE. Since the 1970s, $\delta^{20}\text{Si}_{\text{diatom}}$ values steadily decline and reach the absolute minimum of -0.29 ‰ in the topmost sample (Fig. 2).

1 $\delta^{13}\text{C}$ values are mainly above the mean of -30.6 ‰ before 1950 CE, ranging from -31.1 ‰ at about 1800 CE to the absolute maximum of -29.5 ‰ at ca. 1900 CE (Fig. 2). Since the 1950s, $\delta^{13}\text{C}$ continuously decreases towards more depleted values, including the absolute minimum of -32.3 ‰ at about 2000 CE. The $\delta^{15}\text{N}$ record shows a generally low variability and follows mainly the mean value of $+2.9$ ‰

395 and varies in total by $\pm 0.5\%$, with slightly enriched values between approx. 1930 and 1970 CE and a subsequent minor decline (Fig. 2).

1 The three correlation matrices, which show Pearson correlation coefficients for the total record of the short core EN18232-1 and data from before and after 1950 CE, are displayed in the appendix (Fig. A2–A4).

400 1



1 Figure 2. Biogeochemical records of the short core EN18232-1: Total organic carbon (TOC), total nitrogen (TN), TOC/TN atomic ratio (C/N), organic carbon accumulation rate (OCAR), diatom silicon isotopes ($\delta^{30}\text{Si}_{\text{diatom}}$), as well as stable carbon ($\delta^{13}\text{C}$) and nitrogen ($\delta^{15}\text{N}$) isotope values of bulk sediment

Formatiert: Überschrift 1, Vom nächsten Absatz trennen

Formatiert: Überschrift 1

samples. Vertical lines indicate the mean values. Horizontal lines indicate diatom zones (DZ), the dashed line marks the time before and after 1950 CE.

3

3.23.1 Diatom assemblages and corresponding indices

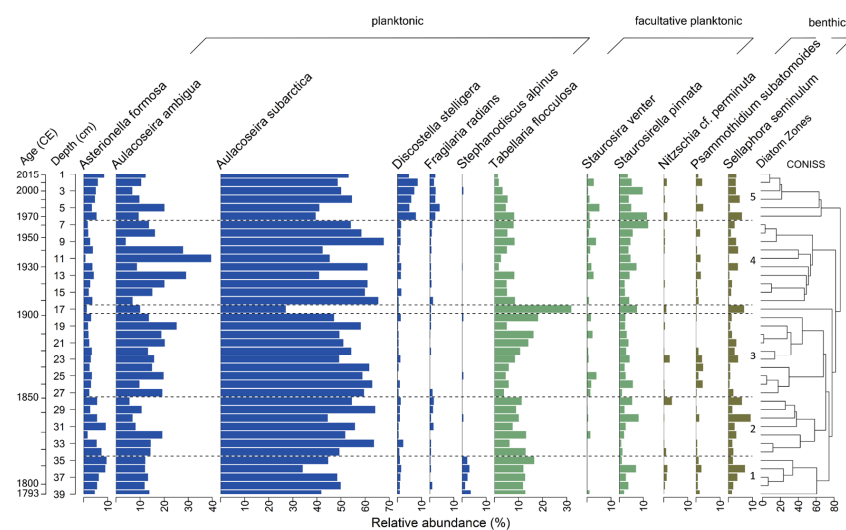


Figure 23. Relative abundances of most dominant diatom species ($\geq 2\%$ in ≥ 2 samples) of the short core EN18232-1 versus sample depth and corresponding mean ages. Diatom zones are based on CONISS clustering shown on the right. Habitat preferences shown at the top.

Diatoms occur in all 39 samples of the short core EN18232-1. In total, 102 species were identified, with 12 species occurring with more than 2 % in ≥ 2 samples (Fig. 3Fig. 2). The valve dissolution F index, not displayed here, reveals overall a good valve preservation within the short core (mean: 0.84; min: 0.71; max: 0.92). The record is dominated by the planktonic *Asterionella*-centric genus *Aulacoseira*, mainly represented by *A. subarctica* and *A. ambigua*, followed by *Tabellaria flocculosa* with a mean abundance of 8.9 %. According to the cluster analysis, we divided the diatom assemblage of EN18232-1 into five diatom zones (Fig. 3Fig. 2). Following percentage values refer to the mean abundance of the individual diatom species within the specific diatom zone. Only the most abundant species ($n=12$) are considered:

Diatom zone 1 (39–35 cm; circa 1790–1815 CE)

The first zone of the diatom record is dominated by the planktonic species *A. subarctica* (43.8 %), followed by the facultatively planktonic *T. flocculosa* (13.2 %) and the planktonic *A. ambigua* (12.7 %). Besides the two *Aulacoseira* species, the planktonic species *Asterionella formosa* (7.0 %), *Discoaster stelligera* (1.2 %), *Fragilaria radians* (0.4 %) and *Stephanodiscus alpinus* (2.5 %) are also represented, at which the latter appears almost only in this diatom zone. Facultative planktonic diatom species are further represented by *Staurosira pinnata* (3.3 %). *Fragilaria cf. gracilis* and *Staurosira venter* have whereby the latter has only low abundance

Formatiert: Schriftart: Kursiv

430 with a maximum of 1 %, ~~whereby the latter appears only once in the lowest sample~~. Overall benthic diatoms are the least represented, especially by *Sellaphora seminulum* (3.2 %), followed by *Psammothidium subatomoides* and *Nitzschia cf. perminuta*.

Diatom zone 2 (34–28 cm; circa 1815–1850 CE)

435 Diatom zone 2 is characterised by the two most abundant species *A. subarctica* (54.8 %) and *A. ambigua* (11.3 %), followed by *T. flocculosa* (10.1 %). *A. formosa* (5.4 %) show a slight decrease. Comparable to diatom zone 1, *S. pinnata* (3.2 %) represent facultative planktonic diatoms and benthic diatoms are mainly represented by *S. seminulum* (3.8 %).

440 Diatom zone 3 (27–17 cm; circa 1850–1910 CE)

In addition to the almost continuous dominance of *A. subarctica* (52.7 %) and *A. ambigua* (16.4 %), *T. flocculosa* shows an increase (11.4 %) and a peak around 1900 CE at the transition to zone 4 (max: 32 %), while both *Aulacoseira* taxa decline at this point. *S. pinnata* (3.5 %) and *S. seminulum* (2.2 %) also show a slight increase towards zone 4. *A. formosa* (2.6 %) continues to decline, while the facultative planktonic species *S. venter* (1.2 %) appears more frequently in this zone.

Diatom zone 4 (16–7 cm; circa 1910–1970 CE)

Dominant planktonic species are represented by *A. subarctica* (55.7 %) and *A. ambigua* (18.1 %), both reaching a maximum in this zone, while *A. formosa* (2.8 %) stays at a reduced level. Facultative planktonic diatoms are represented rather equally by *T. flocculosa* (5.9 %) and *S. pinnata* (5.1 %), the latter reaching a maximum towards zone 5 (max: 12.0 %). Benthic diatoms, *S. seminulum* and *P. subatomoides* show only minor occurrence.

Diatom zone 5 (6–1 cm; circa 1970–2015 CE)

455 The uppermost diatom zone is characterised by a decrease of the two dominant *Aulacoseira* species (*A. subarctica*: 47.9 %; *A. ambigua*: 11.5 %) and a clear increase of the planktonic *D. stelligera* (6.5 %) as well as of *A. formosa* (5.5 %) ~~and *F. radians* (2.6 %)~~. The occurrence of *S. pinnata* (6.5 %) remains elevated ~~and *F. cf. gracilis* (2.6 %) shows a continuous presence~~ in this zone. The abundance of *T. flocculosa* (4.1 %) declines towards the top to its lowest values in the record. Benthic diatoms are still underrepresented mainly based on *S. seminulum* (3.4 %).

460 Indices, derived from the diatom data set, are presented in ~~Fig. 4~~Fig. 3. The diatom valve concentration (DVC) increases towards the top of the core and range from 82.7 to 533.8 10^7 valves g^{-1} , with a mean of 212.2 10^7 valves g^{-1} . This results in a mean diatom valve accumulation rate (DAR) of 464.1 10^9 valves $m^{-2} a^{-1}$ (200.98–1529.6 10^9 valves $m^{-2} a^{-1}$). The rarefied species richness, Hill's N0, has a mean of 21.6 and varies between 13.9 and 27.7. The evenness (effective richness), Hill's N2, result in a mean of 3.3 and span from 2.1 to 6.0. The combined abundance of *A. ambigua* and *A. subarctica*, has a mean of 66.7 % and has a similar curve to the ratio of planktonic–to–benthic diatoms (P/B). Downcore the P/B ratio fluctuate along the mean value of 24.3–6 before it declines to values below the mean after ca. 1950 CE. The *Mallomonas* index (M/D) has a mean of 3.5 and ranges from 0 to a clear maximum of 21.9 in the topmost sample (~~Fig. 4~~Fig. 3).

Formatiert: Schriftart: Kursiv

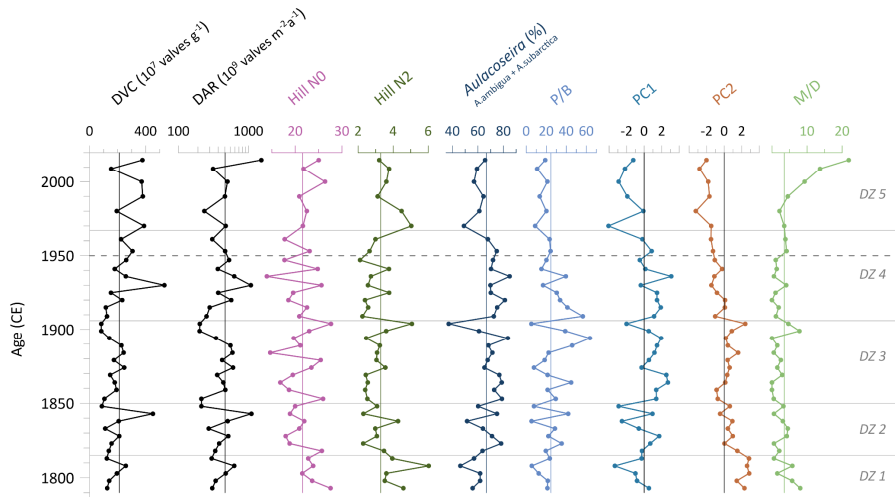


Figure 4.3. Statistical diatom indices of the short core EN18232-1. Diatom valve concentration (DVC), diatom accumulation rate (DAR), diatom species richness (Hill's N0) and evenness (Hill's N2), abundances of *Aulacoseira* species (*A. ambigua* and *A. subarctica*), planktonic-to-benthic species ratio (P/B) of most abundant species excluding tychoplanktonic species, main axis sample scores of principal component analysis (PC1, PC2), and the *Mallomonas* index (M/D). Vertical lines indicate the mean values. Horizontal lines indicate diatom zones (DZ), the dashed line marks the time before and after 1950 CE.

The biplot of sample scores on the first and second axes of the principal component analysis (PCA) of diatom species data explains nearly 45 % of the total variance, whereby PC1 explains 25.7 % and PC2 explains 19.2 % (Fig. 5 Fig. 4). TOC, TN and the *Mallomonas* index (M/D) show association with the diatom species *Staurosirella* *S. pinnata* along the negative axis of PC1 and PC2 and with diatom samples after 1950 CE. Mercury, measured at the same sample material (Stieg et al., 2024b), is affiliated with the diatom species *D. iscostella* *stelligera* and *F. fragilaria* *f. gracilis* *radians* and also points towards samples after 1950 CE. In addition, DVC and DAR point in the same direction, but are both somewhat shorter. The C/N ratio, $\delta^{30}\text{Si}_{\text{diatom}}$ and $\delta^{13}\text{C}$ display opposing clustering to the previous sediment proxies along positive PC1 and PC2 axis. $\delta^{15}\text{N}$ is associated with *Staurosira* *S. venter* and *A. ulacoseira* *subarctica* along the negative PC2 axis. OCAR is positioned along the positive PC2 axis, associated with *Tabellaria* *T. flocculosa* and *Stephanodiscus* *S. alpinus*. $\delta^{18}\text{O}_{\text{diatom}}$ does not exhibit a strong directional association with any particular diatom species.

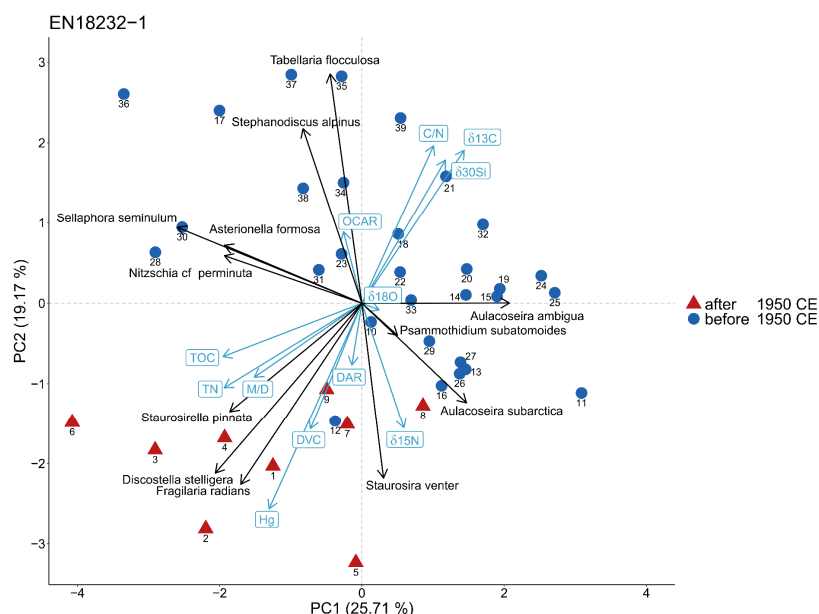


Figure 5-4. Biplot showing the results of the principal component analysis (PCA) with its first two dimensions (PC1, PC2) of the short core EN18232-1 derived from most abundant diatom species data ($\geq 2\%$ in ≥ 2 samples) and corresponding environmental proxies. The percentage of explained variance for each principal component (PC) is displayed on the axis label. Coloured sample depths indicate mean ages before and after 1950 CE.

3.2 Biogeochemical proxies and $\delta^{30}\text{Si}_{\text{diatom}}$

The stratigraphic profiles of TOC and TN show a very similar pattern throughout the core (Fig. 5). The TOC and TN records are strongly intercorrelated ($r = 0.98$, $p < 0.05$; Fig. 2, A2). TOC has a mean value of 9.2 % and TN has a mean of 0.9 %. Around 1800 CE, at the lower part of the core, both proxies are above their mean. Between ca. 1830–1940 CE, values decline and stay below their mean, including their minima at about 1875 CE (TOC = 7.5 %, TN = 0.7 %). At the onset of the 1950s, TOC and TN values rise above the mean again and increase nearly continuously since the 1970s, reaching both their total maxima in the uppermost sample (TOC = 12.5 %, TN = 1.2 %). The C/N ratio has a mean of 12.6 and varies by ± 1.4 . Until the 1950s, the C/N ratio fluctuates slightly between 12.5 and 13, including two maxima at around 1800 CE and 1895 CE. Around 1950 CE, the C/N ratio shifts to lower values of about 12. In the two uppermost samples, the ratio slightly increases again towards 12.5 (Fig. 2 Fig. 5). The values of OCAR fluctuate slightly around the mean value of $20.5 \text{ g m}^{-2} \text{ a}^{-1}$ and only fall below it from the 1950s until a minimum of $11.5 \text{ g m}^{-2} \text{ a}^{-1}$ at around 1970 CE, before rising to the maximum value of $50.6 \text{ g m}^{-2} \text{ a}^{-1}$ in the youngest sample (Fig. 2 Fig. 5).

$\delta^{30}\text{Si}_{\text{diatom}}$ ranges between -0.29 to $+0.52$ ‰, with an overall mean of $+0.24$ ‰. Until 1970 CE, $\delta^{30}\text{Si}_{\text{diatom}}$ values stay mainly above the mean, including the absolute maximum of $+0.52$ ‰ around 1900 CE. Since the 1970s, $\delta^{30}\text{Si}_{\text{diatom}}$ values steadily decline and reach the absolute minimum of -0.29 ‰ in the topmost sample (Fig. 2 Fig. 5).

$\delta^{13}\text{C}$ values are mainly above the mean of -30.6 ‰ before 1950 CE, ranging from -31.1 ‰ at about 1800 CE to the absolute maximum of -29.5 ‰ at ca. 1900 CE (Fig. 2Fig. 5). Since the 1950s, $\delta^{13}\text{C}$ continuously decreases towards more depleted values, including the absolute minimum of -32.3 ‰ at about 2000 CE. The $\delta^{15}\text{N}$ record shows a generally low variability and follows mainly the mean value of +2.9 ‰ and varies in total by ± 0.5 ‰, with slightly enriched values between approx. 1930 and 1970 CE and a subsequent minor decline (Fig. 2Fig. 5). The three correlation matrices, which show Pearson correlation coefficients for the total record of the short core EN18232-1 and data from before and after 1950 CE, are displayed in the appendix (Fig. A2–A4).

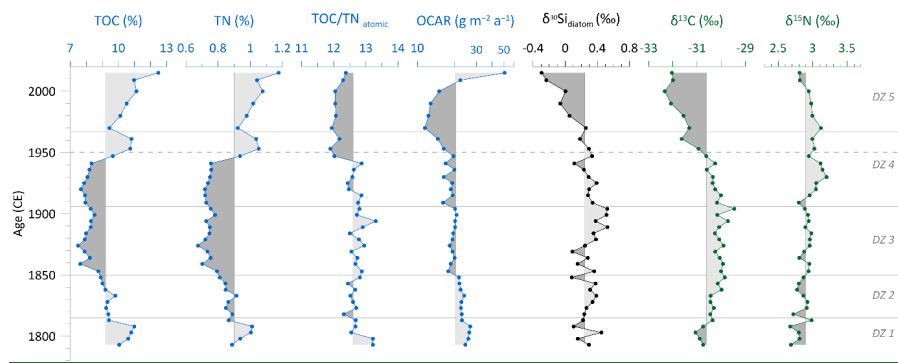


Figure 2.5. Biogeochemical records of the short core EN18232-1: Total organic carbon (TOC), total nitrogen (TN), TOC/TN atomic ratio (C/N), organic carbon accumulation rate (OCAR), diatom silicon isotopes ($\delta^{30}\text{Si}_{\text{diatom}}$), as well as stable carbon ($\delta^{13}\text{C}$) and nitrogen ($\delta^{15}\text{N}$) isotope values of bulk sediment samples. Vertical lines indicate the mean values. Horizontal lines indicate diatom zones (DZ), the dashed line marks the time before and after 1950 CE.

Formatiert: Schriftart: Nicht Kursiv

Formatiert: Standard

4 Discussion

4.1 Limnoecological interpretation of Lake Khamra diatom assemblages

Owing to the deep central part of Lake Khamra (maximum depth: 22.3 m; Fig. 1c), planktonic diatom species have been prominent over the last ~220 years, as reflected by their high abundance within in the short core EN18232-1 (Fig. 3Fig. 2). The planktonic diatom genera *Aulacoseira*, mainly represented by *A. subarctica* and *A. ambigua*, is the most abundant in the sediment record and common in deep, cold, predominantly unstratified lakes in the Arctic tundra (Round et al., 1990; Laing and Smol, 2003). Given its large, highly silicified and thus heavy frustules which rapidly sink (Laing and Smol, 2003), *Aulacoseira* taxa rely on adequate turbulence to stay suspended within the water column (Kilham et al., 1996; Gibson et al., 2003). Thermal stratification or a perennial lake ice cover can weaken the turbulence and lead to a settlement of heavier diatom cells (Gibson et al., 2003). Most *Aulacoseira* species develop dense resting cells as part of their life cycle, which must be resuspended from the sediment into the water column to sustain planktonic populations (Round et al., 1990). Temperature measurements taken under the ice in March 2020 (Biskaborn et al., 2021a) indicate very cold water temperatures at Lake Khamra (mean: 2.5 °C) and a well-mixed water column (Stieg et al., 2024b). Given that *A. subarctica* predominates throughout the record (Fig. 3Fig. 2), it suggests that the growth conditions at Lake Khamra generally favour this species, and a seasonal ice cover does not necessarily reduce its abundance. Furthermore, the snow-rich region and the associated inflow of cold snowmelt water (Stieg et al., 2024b) presumably lead to sufficient turbulence and nutrient upwelling in spring, which likely ensure an promoting sustained enduring circulation beneficial for *A. subarctica* (Horn et al., 2011). However, other factors, including atmospheric-surface temperature gradients and wind-induced mixing, are also likely relevant for sufficient lake overturn (Smol and Douglas, 2007; Winder and Sommer, 2012).

Facultative planktonic species, mainly epiphytic (attached to plants), are less abundant and primarily characterised by *T. flocculosa* (reaching up to 32 %) and *S. pinnata* (up to 12 %; Fig. 3Fig. 2). Besides the deep central part, Lake Khamra has a shallow littoral area (Fig. 1c), where macrophytes are likely find favourable growing conditions that can provide habitat for epiphytic diatom taxa. Purely benthic diatoms (*N. cf. perminuta*, *P. subatomoides*, *S. seminulum*) are of low abundance at Lake Khamra and reach a maximum of 3 % to 9 %. Light limitations due to the lake depth and, annual ice cover, and cold water temperatures, as well as the availability of nutrients likely regulate the abundance of benthic taxa.

The rarefied species richness (mean Hill's N0: 21.6) and evenness (mean Hill's N2: 3.3) are rather low, also suggesting a few species dominate Lake Khamra.

In general, the diatom assemblage of the short core EN18232-1 characterises a deep, open freshwater lake in the boreal forest biome with oligotrophic conditions over the last 220 years. We observe a consistently high diatom valve accumulation rate (DAR) above the minimum of $201 \cdot 10^9$ valves $\text{m}^{-2} \text{a}^{-1}$ indicates continuous diatom accumulations suggest high diatom valve concentration (DVC, mean $212 \cdot 10^2$ valves g^{-1}) within the short core, compared to e.g. a surface sediment lake core from the Siberian Arctic (Biskaborn et al., 2023) or to another pristine lake in Yakutia (Biskaborn et al., 2021b). This likely indicates favourable growth conditions at Lake Khamra that enhance ensures sufficient diatom productivity and good reflect good-preservation environments are reflected, as evidenced by an overall high *F* index (mean: 0.84) of the short core. These factors, along with and the sub-decadal resolution of the record, of the short core make the Lake Khamra well-suited for paleoecological studies.

Formatiert: Hochgestellt

Formatiert: Hochgestellt

Formatiert: Hochgestellt

4.2 Linking diatom assemblage shifts to hydroclimatic and lake environmental changes variability

4.2.1 Diatom zone 1: A reduction of main *Aulacoseira* taxa align with reduced winter precipitation

Based on the cluster analysis, the diatom assemblage of the short core is subdivided into five diatom zones (Fig. 2). The following discussion focuses on major changes within these zones. In diatom zones 1–4 (pre-1970s), assemblage shifts occur mainly in diatom zone 1 (~1790–1815 CE), followed by a rather stable phase until the 1970s.

From the onset of the record until ~1815 CE, in diatom zone 1 (1790–1815 CE), we observe the dominance of the two planktonic diatom genera *Aulacoseira*, mainly represented by the species *A. subarctica* and *A. ambigua*. However, the abundance of *Aulacoseira* is reduced compared to the following was lower than in the subsequent three diatom zones, and remains similarly low as observed in the most recent zone after 1970 CE (Fig. 4 Fig. 3). At the time of diatom zone 1, a hydroclimatic reconstruction from Lake Khamra, reconstructed by using based on a $\delta^{18}\text{O}_{\text{diatom}}$ record of the same sediment samples (Stieg et al., 2024b), indicates a rather dry and cool period at the onset of the record (~1790–1830 CE). This is reflected in elevated $\delta^{18}\text{O}_{\text{diatom}}$ values, suggesting, with reduced winter precipitation (Fig. 6) (Stieg et al., 2024b). It is assumed that less precipitation in winter, accumulated as snow, leads to reduced snowmelt water inflow into the lake. This could lead to reduced water turbulence in spring and hence less favourable conditions for *Aulacoseira* to bloom. Both species richness indices (Hill's N_0 and N_2) are notably higher during *Aulacoseira* reduction, showing a clear distinction between the lowest diatom zone and the subsequent ones. The decline in the dominant *Aulacoseira* species likely reduces competitive pressure, allowing other diatom species to establish and leading to a more diverse diatom assemblage. Noteworthy for the planktonic species is *S. alpinus*, which is primarily present only in the lowermost zone of the diatom assemblage. In contrast, the planktonic species *A. formosa* and *S. alpinus* have thrived during diatom zone 1, whereas the latter occurs only in this zone. *S. alpinus* is reported rarely and appears in oligotrophic lakes with very low water temperatures (Håkansson and Kling, 1989; Krammer et al., 1991), align with the assumed cold conditions at the onset of the record. In terms of nutrients, *Stephanodiscus* has a high demand for phosphorus, although it can still grow under low silica concentrations and limited light (Kilham et al., 1986).

The corresponding genera *Stephanodiscus* prefers high electrical conductivities and high dissolved silica concentrations (Håkansson and Kling, 1989; Pestryakova et al., 2018) and appears globally in fresh as well as slightly saline waters (Håkansson and Kling, 1989). *A. formosa* is reported to have a broad nutrient tolerance range (Rimet et al., 2009; Wang et al., 2012). It is generally associated with nutrient rich waters, as it typically thrives in such conditions but it commonly thrives in nutrient rich lakes (Reynolds et al., 2002; Wang et al., 2012; Rühland et al., 2015). However, it has also been observed to become more abundant as nutrient levels decline (Sivarajah et al., 2016). A reduced meltwater inflow due to overall relatively dry winter conditions could have led to both decreased overturn and a lower input of nutrients, including silica (Si). *Aulacoseira* requires high Si availability for their highly silicified frustules (Laing and Smol, 2003), so a reduction in Si input, combined with weaker turbulence, could have favoured other planktonic species like *S. alpinus* as stronger competitors. Overall, however, diatom accumulation rates (DAR) in the lowest diatom zone are rather low, gradually increasing over time, likely due to the initially cool conditions, a lower lake level at Lake Khamra, supported by a low P/B ratio (Fig. 4 Fig. 3)

Formatiert: Schriftart: Nicht Fett

Formatiert: Schriftart: Kursiv

Formatiert: Schriftart: Kursiv

Formatiert: Schriftart: Kursiv

(Wolin and Stone, 2010), and a proportionally higher nutrient concentration during that phase (Moos et al., 2009), likely beneficial for *S. alpinus* and *A. formosa*.

Facultative planktonic species are primarily represented by epiphytic *T. flocculosa* and *S. pinnata* in diatom zone 1 (Fig. 3Fig. 2). *T. flocculosa* has the second highest abundance in this diatom zone and can occur in both benthic as well as planktonic habitats (Heudre et al., 2021). It implies neutral to slightly acidic and nutrient enriched conditions (Palagushkina et al., 2012; Biskaborn et al., 2023), aligning with an assumed higher nutrient concentration at Lake Khamra during that time. *S. pinnata*, as a synonym basionym of *Fragilaria pinnata* (Guiry and Guiry, 2024), is a small tychoplanktonic diatom (Narancie et al., 2016) and is most common in lakes within northern forests (Pestryakova et al., 2018). A reduced input of snowmelt water and a reduced lake level could have increased littoral habitats at the shallow shore areas of Lake Khamra (Fig. 1c), accompanied by increased water plant growth in summer and, thus, also increase the habitat possibilities for these facultative diatoms. Furthermore, cold conditions might have led to an extensive and long lasting ice cover at Lake Khamra. *S. pinnata* as a small fragilarioid taxon, demonstrates resilience to cold water temperatures and lives in the benthos during lake ice cover (Biskaborn et al., 2012). A prolonged lake ice cover could additionally weaken lake water turbulence and further explain the observed decline in *Aulacoseira* abundance, leading to a settlement of the diatom cells (Gibson et al., 2003). Elevated diatom species richness until 1815 CE (Hill's N0 and N2, Fig. 4Fig. 3), mirror the reduced abundance of the main *Aulacoseira* taxa and the relevance of other diatom species in diatom zone 1.

4.2.2 — After the dry and cold period at the onset of the record, both *Aulacoseira* species show a clear increase in abundance until the 1940s, reaching their most elevated highest abundance of the entire record (Fig. 3). The dominance of *Aulacoseira* is accompanied by a decline also reflected in a decrease in effective species richness, as indicated by declining Hill's N2 numbers (Fig. 3). The $\delta^{18}\text{O}_{\text{diatom}}$ hydroclimatic reconstruction suggests a shift from dry to wet conditions around 1830 CE, followed by a prolonged rather stable period in which the lake water was primarily influenced by snowmelt until 1930 CE (Stieg et al., 2024b). During this hydroclimatically stable phase, constant hydroclimatic conditions and sufficient Diatom zones 2 to 4: *Aulacoseira* dominance linked to melt water inflow

In diatom zone 2 (1815–1850 CE) both *Aulacoseira* species clearly increase in abundance until the 1940s, and together reach up to about 75 % reaching their most elevated abundance of the entire record (Fig. 4Fig. 3), in parallel with the disappearance of *S. alpinus* and a slight reduction of *A. formosa*. The dominance of *Aulacoseira* is also reflected in a decrease in species richness indicated by declining Hill numbers (Fig. 4Fig. 3). *A. formosa* is considered to be a competitor of the two dominant *Aulacoseira* taxa (indicated by the opposite directions in the PCA; Fig. 5Fig. 4), as it prefers similar conditions such as water turbulence to avoid sinking, and enhanced stratification primarily terminates the growth of *A. formosa* (Wang et al., 2012). The hydroclimatic reconstruction suggests a shift from dry to wet at 1830 CE followed by a prolonged rather stable period with the lake water primarily influenced by snowmelt until 1930 CE (Stieg et al., 2024b). A rise in increased snowmelt water input presumably provided lake turbulence in sufficient spring turbulence and a nutrient upwelling, beneficial for *A. subarctica* (Horn et al., 2011). The dominance of *Aulacoseira* is also reflected in a decrease in species richness indicated by declining Hill numbers (Fig. 3). Moreover, a higher meltwater input potentially lowers the lake water conductivity, less favourable for *Stephanodiscus* sp. (Pestryakova et al., 2012). Additionally, sufficient meltwater supply likely stabilised the lake at a higher water level, profitable beneficial for planktonic species, and further supported by an increase of the P/B ratio (Wolin and Stone, 2010) at the onset of diatom zone 2 (Fig. 4Fig. 3).

Formatiert: Standard

Formatiert: Schriftart: Nicht Kursiv

650

655

660

665

670

675

680

685

Around 1935 CE, *Aulacoseira* reached a maximum in abundance (~ 85 %) but subsequently declined to a minimum of ~50 % at ca. 1970 CE (Fig. 3), reflecting a period of high variability. This corresponds to a phase of hydroclimatic instability, as indicated by meteorological data from the nearest weather station in Vitim, which In diatom zone 3 (1850–1910 CE) the dominance of *Aulacoseira* stabilises (Fig. 4Fig. 3), further displacing *A. formosa* (Fig. 3Fig. 2), displayed in the rather low level of effective species richness (Hill's N2, Fig. 4Fig. 3). *T. flocculosa* thrives in diatom zone 3 and reaches an absolute maximum (32 %) around 1900 CE, while *Aulacoseira* reaches an absolute minimum (37 %) in one sample. This shift is potentially a reaction to unstable habitat conditions of *T. flocculosa* (Palagushkina et al., 2012), such as transient hydrological changes that had short-term consequences for both planktonic and benthic diatom habitat conditions (Rühland et al., 2015; Biskaborn et al., 2023). A study of a Canadian lake indicates that some taxa, including *T. flocculosa*, show a significant increase with fire disturbance, while planktonic taxa decrease (Philibert et al., 2003). This pattern suggests a similar response in Lake Khamra, where evidence of wildfires around 1880 CE in the lake vicinity (Glückler et al., 2021), marked by a peak in charcoal (Fig. 6), likely caused a short-term disturbance in environmental conditions. Light limitations due to surface and dispersed particles, as suggested by Philibert et al. (2003), could be one possibility, leading to increased growth of *T. flocculosa* and a concurrent decrease in *Aulacoseira*. However, as this shift is based on only a single sample, it should be interpreted with caution.

S. venter establishes in diatom zone 3 and also *S. pinnata* stays at a rather constant abundance, however both remaining on a low level (Fig. 3Fig. 2). Both are small fragilarioid taxa, which are adapted to short growing phases and known as pioneering and opportunistic species, occurring in oligotrophic neutral to alkaline lakes (Biskaborn et al., 2012; Pestryakova et al., 2012; Narancie et al., 2016). Their presence coincides with the dominant influence of winter precipitation on the lake water, which tends to create difficult growing conditions for epiphytic diatoms. Diatom zone 4 (1910–1970 CE) is still characterised by a high abundance of *Aulacoseira*, but clearly decreasing from a maximum at ca. 1935 CE (ca. 85 %) to a minimum at ca. 1970 CE (of ca. 50 %; Fig. 4Fig. 3), indicating high variability. Meteorological data from the nearest weather station in Vitim, starting in the 1930s, suggesting a prolonged annual precipitation deficit (Fig. 6), especially particularly in early winter months precipitation around the 1950s. This further, aligning with a variable hydroclimatic phase including a reconstructed dry anomaly in the 1950s based on the $\delta^{18}\text{O}_{\text{diatom}}$ values around the 1950s (details given in Stieg et al., 2024b) and coincides with and an increased in wildfire activity in the vicinity of the lake, as inferred from a charcoal record from Lake Khamra (Glückler et al., 2021). A reduction of turbulence spring overturn, caused by reduced snowmelt water supply during spring bloom, seems a reasonable explanation for the decline of *Aulacoseira*.

PC1 reaches a minimum associated with the decrease of *Aulacoseira* species (Fig. 4Fig. 3). Comparable to the transition from diatom zone 1 to 2, we simultaneously observe an increase in diatom species richness and especially in evenness between 1950 and 1970 CE (Hill numbers's N2, Hill's N2 peak in the 1970s; Fig. 4Fig. 3). This pattern coincides with the decline of the dominant *Aulacoseira* taxa, likely allowing other diatom species, like facultative planktonic *T. flocculosa* or *S. pinnata* to compete more successfully, which mirrors the reduced abundance of the main *Aulacoseira* taxa and the relevance of other diatom species indicates a shift towards better habitat conditions in favour of epiphytic and benthic diatoms. A reduction in precipitation likely led to a decreased lake level, thereby increasing littoral habitats and macrophyte growth in the shallow shore areas of the lake, contributing to a more complex diatom community.

Formatiert: Schriftart: Kursiv

Formatiert: Schriftart: Kursiv

690 Facultative planktonic diatoms remain relatively constant, except for *S. pinnata*, which shows a maximum around 1970 CE (Fig. 3 Fig. 2), which could be a response to increased fire activity. There are reports that certain diatom species, such as *Fragilaria pinnata*, *F. construens* var. *venter*, and *Tabellaria quadrisepitata*, become more abundant during fire intervals (Rühland et al., 2000), based on a peat core analysis in Siberia (Jasinski et al., 1998), linked to enhanced weathering and increase silt deposition (Rühland et al., 2000).

4.2.34.2.1 Diatom zone 5: Diatom shift at 1970 CE: A climate warming signal

700 The most prominent shift in diatom assemblage occurs around 1970 CE, corresponding to marking the transition between diatom zones 4 and 5. We observe a significant major shift in diatom assemblage at 1970 CE, separating diatom zones 4 and 5 (Fig. 3 Fig. 2). Diatom zone 5 (~1970–2015 CE) is characterised by a significant substantial increase in the planktonic *D. stelligera*, rising from low relative abundances up to 8.5 %, while both *Aulacoseira* species show a minimum (Fig. 6). *D. stelligera* (~~synonym~~ ~~basionym~~ *Cyclotella stelligera*; (basionym *Cyclotella stelligera*; Guiry and Guiry, 2024), belongs to diatoms of the *Cyclotella sensu lato* taxa (Saros and Anderson, 2015). The shift in diatom assemblage characterised by an increase of small cyclotelloid planktonic diatoms like the *Cyclotella stelligera* complex and a simultaneously decrease of *Aulacoseira* taxa and/or small benthic fragilarioid taxa is revealed in other paleolimnological studies ~~on from~~ the northern hemisphere (Rühland et al., 2003; Smol et al., 2005; Rühland et al., 2008). Diatom zone 5 corresponds with a hydroclimatic phase of the $\delta^{18}\text{O}_{\text{diatom}}$ record, indicating increased winter precipitation and more snowmelt water supply to in Lake Khamra, as supported by meteorological data (Fig. 6) (Stieg et al., 2024b). Despite increased water turbulence from inflow, which usually benefits *Aulacoseira*, its observed decrease is unexpected. Therefore, we infer that an additional factor is responsible for the decline. ~~In Since~~ the 1970s regional annual temperature start to increase (Anomalies of annual mean temperature, Vitim; Fig. 6). Rising temperatures, in the context of global warming, likely reduce the ice-cover duration and increases the possibility of thermal stratification of the lake water in the ice-free period, which allowing *D. stelligera* to thrive (Smol et al., 2005; Rühland et al., 2015). Increased summer stratification is, less favourable for *Aulacoseira* (Gibson et al., 2003; Rühland et al., 2008), although it remains dominant at Lake Khamra (>50 %, Fig. 4 Fig. 3).

720 ~~In the same sediment samples~~ Additionally, we observe a significant rapid increase in the silicified chrysophyte *Mallomonas scales* since the 1990s, inferred from the *Mallomonas* index (M/D) (Fig. 4 Fig. 3). Chrysophytes are common in oligotrophic environments (Smol, 1985). Their motility, enabled by flagella, allows them to thrive in stratified lakes by maintaining their position in the photic zone. This gives them an advantage over non-motile, colonial diatoms such as *Aulacoseira* (Ginn et al., 2010; Mushet et al., 2017). The observed increase in chrysophytes at Lake Khamra suggests changes in the lake's mixing regime. ~~F, and further it provides evidence for a likely longer ice-free period and enhanced thermal stratification during summer months in recent decades. Similar increases in scaled chrysophytes have been reported in other lake systems, associated with climate warming and increased thermal stability~~ (Paterson et al., 2004; Ginn et al., 2010; Favot et al., 2024).

725 ~~An increase of annual temperature and a shorter lake ice period extend the diatom growing season and change light and nutrient availability, favouring small planktonic diatoms (Rühland et al., 2015). Observed elevated diatom species richness (Hill's N0, Fig. 4 Fig. 3) are congruent with reported increased diatom community complexity and diversity during prolonged ice-free periods in Arctic lakes (Douglas and Smol, 2010; Rühland et~~

Formatiert: Schriftart: Nicht Fett

Formatiert: Schriftart: Kursiv

Feldfunktion geändert

730 al., 2015). During longer ice-free periods, the shallow littoral zones of Lake Khamra would be more exposed to
 sunlight, accelerating water heating and potentially offering better conditions for water plants to thrive. Increased
 macrophyte growth likely change the nutrient availability and offer new habitat for epiphytic diatoms, like *S.*
pinnata or *F. cf. gracilis* (which establish in diatom zone 5, Fig. 3Fig. 2). Different studies have reported a rise in
 pennate (tychoplanktonic) planktonic *Fragilaria* populations as a response to climate warming (Rühland et al.,
 735 2013; Michelutti et al., 2015; Sochuliakova et al., 2018). *S. pinnata* and *F. cf. gracilis* both groupplot
 together with *D. stelligera* in the PCA biplot (Fig. 5Fig. 4), and *F. radians* also occur primarily in the uppermost
 diatom zone (Fig. 2), underlining a possible common reaction to warming at Lake Khamra.

In many Arctic lakes, comparable shifts in the diatom community occurred as early as 1850 CE (Smol et al., 2005),
 while the change at Lake Khamra occurred about 120 years later. The timing discrepancy regarding the onset of
 740 increase in small *Cyclotella sensu lato* species aligns precisely with studied temperate regions in North America
 and Europe (Rühland et al., 2008), which also show a change from 1970 CE onwards. Siberian-Yakutian lakes are
 rare in circumpolar studies (Smol et al., 2005; Rühland et al., 2008). Nevertheless, a similar shift in diatom
 composition has been observed at Lake Bolshoe Toko, a comparable remote boreal lake in eastern Siberia, after
 1850 CE, interpreted as a response to climate warming (Biskaborn et al., 2021b). However, the much lower
 745 stratigraphic resolution at Lake Bolshoe Toko introduces age uncertainties, making direct comparison with the
 Lake Khamra record difficult. The observed age offset in diatom shifts could refer toindicate different climate
 related driverst-phases-of-climate-warming. Furthermore, analogous observations were-madediatom assemblage
 shifts are observed at the south basin of Lake Baikal at ca. 1970 CE (Roberts et al., 2018), as well as at pristine
 Arctic and sub-Arctic lakes in the northern Urals with most distinct shifts after 1970 CE (Solovieva et al., 2008).
 750 Our data align with the later onset of diatom assemblage changes at lower latitudes compared to the earlier changes
 observed in Arctic regions, which is attributed to an earlier warming and a quicker response of Arctic ecosystems
 compared to lower latitudes (Smol et al., 2005; Smol and Douglas, 2007).

An increase of annual temperature and a shorter lake ice period extend the diatom growing season and change
 light and nutrient availability, favouring small planktonic diatoms (Rühland et al., 2015). Observed elevated
 755 diatom species richness (Hill's N0, Fig. 4) are congruent with reported increased diatom community complexity
 and diversity during prolonged ice-free periods in Arctic lakes (Douglas and Smol, 2010; Rühland et al., 2015).
 During longer ice-free periods, the shallow littoral zones of Lake Khamra would be more exposed to sunlight,
 accelerating water heating and potentially offering better conditions for water plants to thrive. Increased
 macrophyte growth likely change the nutrient availability and offer new habitat for epiphytic diatoms, like *S.*
 760 *pinnata* or *F. cf. gracilis* (which establish in diatom zone 5, Fig. 3). Different studies have reported a rise in pennate
 (tychoplanktonic) planktonic *Fragilaria* populations as a response to climate warming (Rühland et al., 2013;
 Michelutti et al., 2015; Sochuliakova et al., 2018). *S. pinnata* and *F. cf. gracilis* both plot together with *D. stelligera*
 in the PCA biplot (Fig. 5), underlining a possible common reaction to warming at Lake Khamra.

The shifts in diatom assemblage delineating zones 4 and 5 as well as 1 and 2 have similarities (*Aulacoseira* decline
 765 while planktonic cyclotelloid taxa such as *S. alpinus* or *D. stelligera* increase and diatom richness increase).
 However, we also see clear differences (cold habitat preferences from *S. alpinus* vs. warm and stratified
 preferences of *D. stelligera*, increase of *F. cf. gracilis* and *S. pinnata* in recent years only) which suggests
 that the increase in air temperatures in recent decades significantly notably influenced the lake ecosystem and its
 diatom assemblages, overprinting the influence of a simultaneous precipitation increase.

Feldfunktion geändert

Formatiert: Schriftart: Kursiv

Feldfunktion geändert

Formatiert: Schriftart: Kursiv

Feldfunktion geändert

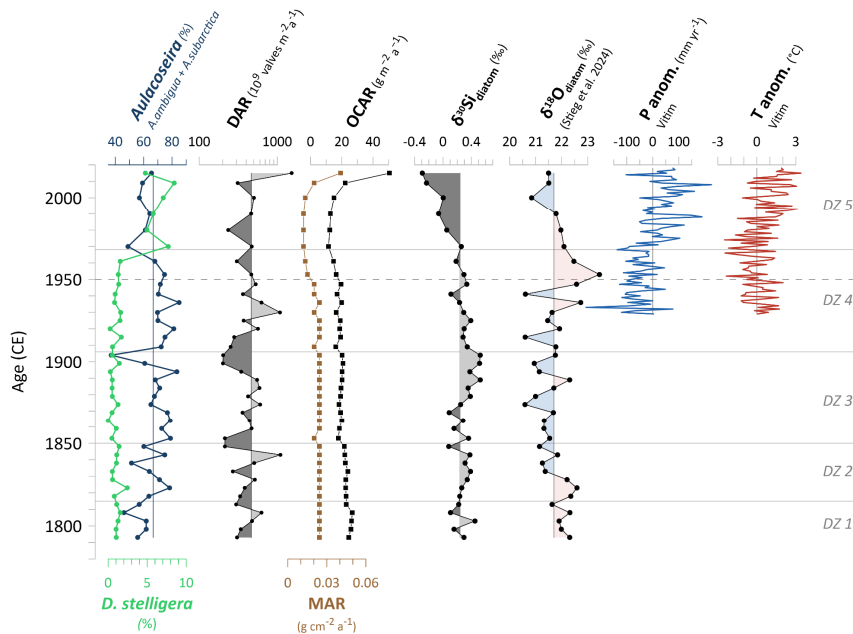


Figure 6. Comparable records as possible forcing for diatom assemblage changes and selected biogeochemical proxies in relation to hydroclimatic variability: *Aulacoseira* vs. *D. stelligera* abundances of the short core EN18232-1; diatom accumulation rates (DAR); mass accumulation rates (MAR) and carbon accumulation rates (OCAR); $\delta^{30}\text{Si}_{\text{diatom}}$ record; $\delta^{18}\text{O}_{\text{diatom}}$ record from the same short core of Lake Khamra (Stieg et al., 2024b); Anomalies of annual mean temperature and annual precipitation from the weather station in Vitim (59.45° N, 112.58° E; 186 m a.s.l.; ECA (European Climate Assessment); data accessible via the KNMI Climate Explorer <https://climexp.knmi.nl>; last access: 15. July 2024; (Klein Tank et al., 2002); NOAA Climate Data Record of Total Solar Irradiance (TSI, (Coddington et al., 2015); charcoal record from Lake Khamra, "classic" and "robust CHAR", letter accounts for accumulated uncertainties (Glückler et al., 2024). Vertical lines indicate the individual mean values. Horizontal lines indicate diatom zones (DZ), the dashed line marks the time before and after 1950 CE.

Formatiert: Hochgestellt

Formatiert: Tiefgestellt

4.3 Biogeochemical proxies as indicators of bioproductivity and ~~erosion~~ organic matter sources at Lake Khamra

4.3.1 Biogeochemical shifts after 1950 CE

Carbon and nitrogen indicators (TOC, TN, C/N, OCAR, $\delta^{13}\text{C}$; ~~Fig. 2~~Fig. 5) show a notable shift at 1950 CE, highlighting substantial limnological changes that precede the major shifts in diatom communities observed starting at 1970 CE (onset of diatom zone 5). We propose that hydroclimatic variability ~~substantially~~significantly influences limnological conditions at Lake Khamra, with some diatom species responding immediately. However, the ~~most ecologically important~~broader shift in the diatom assemblage appears to occur ~~later~~~1970 CE and is more likely driven by rising temperatures and their associated limnological effects, as discussed above.

At ~1950 CE, the $\delta^{18}\text{O}_{\text{diatom}}$ values reach a maximum (Fig. 6), interpreted as a dry anomaly with reduced input of isotopically light winter precipitation into the lake (Stieg et al., 2024b). This reconstructed ~~dry~~anomaly aligns with the overall dry period inferred from persistently below-average annual precipitation starting from the 1930s, at the onset of meteorological recordings, and continuing until the 1970s (Fig. 6; details in Stieg et al., 2024b). Additionally, a charcoal record from the same lake identifies enhanced fire activity during the 1950s (Glückler et al., 2021), coinciding with the $\delta^{18}\text{O}_{\text{diatom}}$ maximum, providing further evidence of this dry anomaly. At the same time, mass accumulation rates (MARs) drop (Fig. 6), which could be linked to a reduction in erosional input, further supported by the flattening of the age-depth relationship from the 1950s onwards (Fig. A1), indicating lower sedimentation rates. The concurrent decrease in organic carbon accumulation rate (OCAR) to a minimum of $11.5 \text{ g m}^{-2} \text{ a}^{-1}$ between 1950 and 1970 (Fig. 5 & 6) suggests lower erosional input of organic material, a reduced primary productivity, or a combination of both. In addition to the dry phase, declining annual temperatures, reaching a minimum between ~1950 and 1970 CE (Fig. 6), indicate simultaneously cool conditions. While *Aulacoseira* remains dominant, it decreases especially between the 1950s and the 1970s. Diatom accumulation rates (DARs) decline after the peak in the 1930s indicating rather a reduction in primary productivity around the 1950s. This is likely linked to cold annual temperature anomalies and less nutrient refreshment due to reduced turbulence and inflow, as *Aulacoseira* begins to decline. It is probable that during the dry period with less snowmelt inflow during the 1950s, as deduced by Stieg et al. (2024b), the erosional input from catchment is reduced, aligning with a low sedimentation rate during that time (also visible in the flattening of the age-depth relationship starting in the 1950s; Fig. A1). Concurrently, the accumulation rate of organic carbon (OCAR) declines to a minimum of $11.5 \text{ g m}^{-2} \text{ a}^{-1}$ from 1950 to 1970 CE (Fig. 2Fig. 5), aligning with the decrease of the most abundant diatom taxa *Aulacoseira* at the end of diatom zone 4. In contrast, total organic carbon (TOC) and total nitrogen (TN), which represent the fraction of organic matter and are closely related to primary productivity (Meyers and Teranes, 2001), both show a peak between 1950 and 1970 CE (Fig. 2Fig. 5), indicating higher bioproductivity. It is plausible, that low sedimentation rates could result in a relative increase in TOC and TN concentrations within the sediment, explaining the contrasting tendency.

We observe a similar trend in rising DVC and rather stable DAR (Fig. 4Fig. 3). The increase in DVC above the mean since the 1950s, indicating a shift towards enhanced diatom productivity, could potentially be linked to the increasing diatom richness (rising Hill numbers, Fig. 4Fig. 3) due to habitat changes as the dominant *Aulacoseira* decline. Alternatively, the higher DVC could also be attributed to low sedimentation rates, increasing its concentration. The high *F*-index (mean: 0.84) supports that preservation is consistently very good across all sediment layers, indicating no significant taphonomic changes affecting the diatom signal.

Formatiert: Tiefgestellt

During the dry period between the 1950s and 70s, the erosional input from the catchment was probably reduced. However, a differentiation between autochthonous (in-lake) or allochthonous origin of organic material since then remains indistinct. The atomic organic carbon-to-nitrogen ratio (C/N) together with $\delta^{13}\text{C}$ help to identify the organic matter origin (Meyers, 2009). C/N drops from ca. 13 to a slightly lower level of around 12 since the 1950s, reflecting a mixed signal in both cases. According to the literature, lacustrine algae have a C/N ratio ranging between 4 and 10, whereas organic matter from land plants have a ratio >20 (Meyers and Teranes, 2001). Also together with $\delta^{13}\text{C}$, a differentiation still remains inexplicit (Fig. A57), as both, algae and C_3 -land plants, have similar $\delta^{13}\text{C}$ signatures, making them indistinguishable (Meyers, 2009). The $\delta^{15}\text{N}$ data underlines a mixed organic origin, as the value of 3 ‰ lies in between land plants (around 0 ‰) and freshwater algae (5–10 ‰, (Meyers, 2009). However, the rather low C/N values tend towards an autochthonous organic matter source since the 1950s, underlining a reduced inflow from the catchment.

After 1970 CE, during diatom zone 5, ~~increasing annual precipitation in~~precipitation in the region ~~increases~~ (Fig. 6) ~~and offer the possibility for an-~~suggests an increased erosional input from the catchment. Simultaneously, we observe an increase in both TOC and TN , ~~reaching values of up to 12.5 % and 1.2 % respectively (Fig. 2Fig. 5)~~, pointing towards a higher bioproductivity (Meyers and Teranes, 2001). Since OCAR increases ~~simultaneously at the same time (Fig. 2Fig. 5)~~, it supports an enhanced accumulation of TOC from 1970 CE onwards. ~~However, whereby the C/N ratio in combination with $\delta^{13}\text{C}$ still mirrors a mixed signal of its origin (Fig. 7). The concentration of diatom valves (DVC) remains elevated past 1970 CE (Fig. 2), aligning with the appearance of *D. stelligera* in 1970 CE and the increase in (tycho) planktonic diatom taxa in diatom zone 5. The DAR lags slightly behind and increases after the 1980s (Fig. 6), indicating higher a tendency towards enhanced diatom productivity likely related to warming (Douglas and Smol, 2010; Biskaborn et al., 2012; Biskaborn et al., 2021b). Since diatoms are photosynthetic algae that depend on sunlight, the modern solar maximum around the 1950s and overall elevated insolation since then (Fig. 6) certainly also promoted algae growth.~~

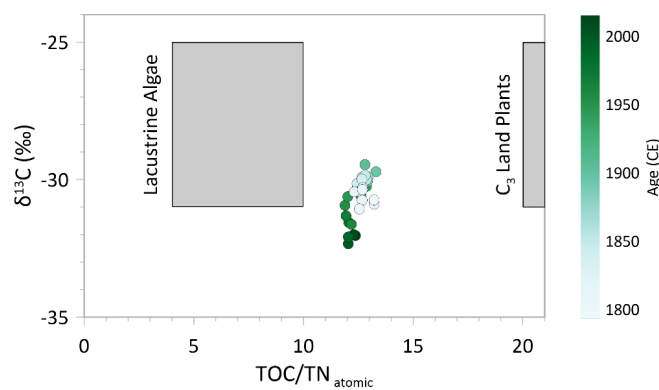


Figure 7. C/N- $\delta^{13}\text{C}$ -plot showing sediment samples of the short core EN18232-1. In general, lacustrine algae have a C/N ratio between 4 to 10, C_3 land plants have a ratio >20 (Meyers and Teranes, 2001). Figure is based on the values given by Meyers and Teranes (2001).

Formatiert: Zentriert

Formatiert: Beschriftung

Formatiert: Tiefgestellt

The continuous decrease in $\delta^{13}\text{C}$ especially since the 1950s (Fig. 2Fig. 5) initially appears to contradict the interpretation of increased bioproductivity in the upper part of the record, even though algae and land plants have similar signatures (Meyers, 2009). In general, phytoplankton preferentially incorporates lighter ^{12}C than ^{13}C , which enriches the remaining reservoir over time and lead to increasing $\delta^{13}\text{C}$ values of organic matter during enhanced productivity (Meyers, 2009). The observed $\delta^{13}\text{C}$ decline might, at least partly, be related to fossil fuel combustion and biomass burning, which release CO_2 depleted in ^{13}C into the atmosphere, known as *Suess effect* (Keeling, 1979). As the CO_2 in the atmosphere and in the water tend to reach equilibrium, this also effects the $\delta^{13}\text{C}$ values of lake sediment organic matter (Verburg, 2007), as observed e.g. in a lake study in West Greenland (Stevenson et al., 2021). Most of the decline in $\delta^{13}\text{C}$ of about 1.7 ‰ at Lake Khamra could, thus, be explained by the decline in atmospheric $\delta^{13}\text{C}$, which has accelerated particularly after 1950 and has fallen by about 1 ‰ since then (Verburg, 2007). In a previous study, increased mercury concentrations indicated that Lake Khamra is affected by human air pollution (Stieg et al., 2024b), further confirmed by a strong correlation between $\delta^{13}\text{C}$ and mercury after 1950 CE ($r = -0.97$, $p < 0.05$, Fig. A4). Aside from that, an increased algae productivity might not contradict with decreasing $\delta^{13}\text{C}$ values, as light CO_2 can be constantly assimilated during increased growth, as observed in an Arctic lake (Jiang et al., 2011).

Like As with $\delta^{13}\text{C}$, $\delta^{30}\text{Si}_{\text{diatom}}$ also shows a decline-decreases, but slightly later at around 1970 CE (Fig. 2Fig. 5 & 6), which coincidinges with the shift of the diatom assemblages between diatom zones 4 and 5. We assume that the decrease in $\delta^{30}\text{Si}_{\text{diatom}}$ is influenced by multiple factors, as the interpretation of silicon isotopes is complex and involves various processes (Sutton et al., 2018). Overall, the $\delta^{30}\text{Si}_{\text{diatom}}$ values are low (mean: $+0.24$ ‰), comparable to e.g. a study at a groundwater-dominated Swedish lake (Zahajská et al., 2021a). Groundwater inflow could lead to low isotope values of dissolved silica (DSi, $\delta^{30}\text{Si}_{\text{DSi}}$) and hence to low $\delta^{30}\text{Si}_{\text{diatom}}$ (Opfergelt et al., 2011; Frings et al., 2016; Zahajská et al., 2021b; Zahajská et al., 2021a). Unfortunately, there is no information on lake water $\delta^{30}\text{Si}_{\text{DSi}}$ or groundwater inflow at Lake Khamra. It is likely that groundwater input at Lake Khamra contributes to the generally low $\delta^{30}\text{Si}_{\text{diatom}}$. However, a sudden change in groundwater seems unlikely and cannot explain the distinct decrease at around 1970 CE.

Fractionation of silicon isotopes occurs through both inorganic chemical weathering and biological activities, mainly diatom growth in marine and terrestrial environments (Opfergelt et al., 2011). In marine environments, diatom silicon utilisation is linked with the silicon isotope composition (De la Rocha et al., 2000; Varela et al., 2004; Cardinal et al., 2005; De La Rocha, 2006), whereas studies in lacustrine environments are sparse. There are studies linking diatom blooms in lakes with silicon isotope fractionation by seasonal *in situ* measurements to validate $\delta^{30}\text{Si}_{\text{diatom}}$ as a bioproductivity proxy (Alleman et al., 2005; Opfergelt et al., 2011; Panizzo et al., 2016).

In this context, $\delta^{30}\text{Si}_{\text{diatom}}$ is used as a paleoenvironmental proxy in only a few paleolimnology studies in Asia, for example at Lake El'gygytgyn in North East Siberia (Swann et al., 2010), or in South China (Chen et al., 2012).

Diatoms preferably incorporate light ^{28}Si instead of heavier ^{30}Si (and ^{29}Si) during biomineralization (De La Rocha et al., 1997; Leng et al., 2009). Assuming this fractionation dominates the isotopic signal of the diatoms at Lake Khamra, the decrease of $\delta^{30}\text{Si}_{\text{diatom}}$ to values of -0.53 ‰ in recent decades contradicts the discussed tendency towards higher algae productivity in diatom zone 5. Higher bioproductivity increases DSi utilisation and would result in both, an enrichment of the DSi signature of the reservoir (lake water) and of the diatom frustules therein. In unlimited lake systems, such as Lake Khamra, alteration of DSi sources can influence $\delta^{30}\text{Si}_{\text{diatom}}$ (Zahajská et al., 2021b), and may overprint the isotopic effect of bioproductivity. We argue-suggest that substantial changes in the catchment have led to significant isotopic changes in the reservoir (lake water), which dominate-influenced the

Formatiert: Schriftart: Kursiv

895 $\delta^{30}\text{Si}_{\text{diatom}}$ record at Lake Khamra. Since 1970 CE, both temperature and precipitation increase in the region (Fig. 6), forcing enhanced weathering in the catchment and e.g. leading to a higher nutrient inflow to the lake (Douglas and Smol, 2010), as supported by the increase in OCAR (Fig. 2 Fig. 5). In addition, the recent wet and warm period at Lake Khamra follows an earlier cold and dry period around the 1950s with increased wildfire activity in the region (Glückler et al., 2021; Stieg et al., 2024b). Fires in the catchment area have likely altered vegetation and soil conditions, consequently affecting the source of dissolved silica. Soils and terrestrial plants, which tend to have low $\delta^{30}\text{Si}_{\text{DPS}}$ values (Frings et al., 2016; Sun et al., 2018), may be subject to increased erosion following the (partial) loss of the vegetation cover. Additionally, Lake Khamra lies within a sporadic permafrost zone (Fedorov et al., 2018). Observed warming could increase the depth of the active layer, which as it thaws, would also preferably transport low $\delta^{30}\text{Si}_{\text{DPS}}$ from litter and soil material into the lake.

905 Besides the change of catchment supply, an alteration of species composition driven by variations in summer temperatures and the duration of ice-free periods (Zahajská et al., 2021b) could further influence $\delta^{30}\text{Si}_{\text{diatom}}$. It remains uncertain if a species effect leads to a different silicon isotope fractionation. While Sutton et al. (2013) provided evidence of such effects in marine diatoms, Schmidbauer et al. (2022) observed varying $\delta^{30}\text{Si}_{\text{diatom}}$ values in lacustrine samples, which were associated with different preferred habitat regimes. We hypothesise, the $\delta^{30}\text{Si}_{\text{diatom}}$ -decrease at Lake Khamra could hence partially mirror the major shift in diatom assemblage changes since the 1970s, from heavy and compact *Aulacoseira* taxa to less silicified *D. stelligera* and smaller tychoplanktonic and benthic taxa, which have less silicon incorporated.

910 Overall, interpreting $\delta^{30}\text{Si}_{\text{diatom}}$ in lacustrine systems is more complex than in marine environments. At Lake Khamra, $\delta^{30}\text{Si}_{\text{diatom}}$ appears to be influenced by multiple factors, including shifts in diatom assemblages and catchment alterations that affect silica sources and utilisation. At Lake Khamra, we consider $\delta^{30}\text{Si}_{\text{diatom}}$ to be an indicator of weathering rather than of diatom productivity.

Formatiert: Tiefgestellt

4.3.2 Biogeochemical shifts trends before 1950 CE

Before 1950 CE we observe a prolonged, rather stable period in most biogeochemical proxies (TOC, TN, C/N, OCAR, $\delta^{13}\text{C}$, $\delta^{30}\text{Si}_{\text{diatom}}$, $\delta^{15}\text{N}$; Fig. 2 Fig. 5) characterised by a dominance of *Aulacoseira* in diatom zones 2, 3 and 4. The sediment $\delta^{13}\text{C}$ values reach up to -30 ‰ and presumably were not substantially influenced by human air pollution prior 1950 CE at Lake Khamra (Verburg, 2007). The slightly elevated C/N ratio of around 13 in combination with the elevated $\delta^{13}\text{C}$ values (Fig. 7) still indicates a mixed source signal of organic material, in combination with the $\delta^{13}\text{C}$ values (Fig. A57) as outlined above. However, compared to the period after 1950 CE, the older section of the record shows there is a tendency towards a more allochthonous origin of the organic material (Meyers, 2009), which could indicate either lower lake-internal productivity or increased erosional inflow of organic matter. Only a few species dominated the record at this time (lowest Hill's N2; Fig. 3), mainly represented by the two *Aulacoseira* taxa. TOC and TN values show their lowest concentration between ~1830 and 1950 CE (Fig. 5), suggesting a reduced bioproductivity (Meyers and Teranes, 2001). OCAR values are less indicative and remain relatively constant until the 1950s (Fig. 5), with DAR showing similar stability, though with some dips indicating periods of lower accumulation (Fig. 6). These trends point to a relatively constant or slightly decreased bioproductivity. As referred from the $\delta^{18}\text{O}_{\text{diatom}}$ record (Fig. 6) (Stieg et al., 2024b), the hydroclimatic conditions were rather stable since ~1830 CE, likely with sufficient. On the one hand, there was probably an increased erosional inflow from the catchment by snowmelt. This rather wet period could explain the tendency towards an

Formatiert: Nicht Hochgestellt/ Tiefgestellt

Formatiert: Hochgestellt

Formatiert: Nicht Hochgestellt/ Tiefgestellt

Formatiert: Schriftart: Kursiv

allochthonous origin of organic material due to the higher (winter) precipitation during a rather stable hydroclimatic phase starting in the 1830 CE (Stieg et al., 2024b). On the other hand, only a few species dominated the record at this time (Hill's N2; Fig. 4Fig. 3) and overall low diatom concentrations (DVC) as well as low diatom accumulation rates (DAR; Fig. 4Fig. 3) suggest a reduced lake productivity in comparison with recent decades. Aligned TOC and TN values show their lowest concentration between 1830 and 1950 CE (Fig. 2), indicating reduced bioproductivity (Meyers and Teranes, 2001).

In contrast to low DVC and DAR, observed $\delta^{30}\text{Si}_{\text{diatom}}$ would suggest enhanced bioproductivity based on the classical interpretation of this proxy (De La Rocha et al., 1997). *Aulacoseira* has a high demand of dissolved silica for their heavy and thick frustules, which could have led to a moderate $\delta^{30}\text{Si}$ enrichment of the reservoir during phases of diatom blooms, but this is likely a minor effect. Furthermore, we assume that, in contrast to the post-1950s period, the catchment was not yet affected by strong wildfire disturbances, leading to a difference in the isotopic signature of pre and post 1950s which led to a different source signal pre 1950 CE and hence less weathering and erosional input of soil and plant material with low $\delta^{30}\text{Si}_{\text{DSS}}$ values is likely. Less influence of isotopic light $\delta^{30}\text{Si}$ plant material from soil erosion. This potentially resulted in a higher $\delta^{30}\text{Si}$ level of dissolved silica, which is reflected in the overall elevated $\delta^{30}\text{Si}_{\text{diatom}}$ (Fig. 6). This highlights the complexity of $\delta^{30}\text{Si}_{\text{diatom}}$ as a proxy, linked likely to both in-lake biogeochemical processes and catchment dynamics at Lake Khamra, and almost constant C/N ratio (Fig. 2Fig. 5). Furthermore, $\delta^{30}\text{Si}_{\text{diatom}}$ seems rather unaffected by diatom assemblage changes or hydroclimatic variability in the lower part of the core before 1950 CE (as no correlation is observed to any other proxy; Fig. A3), supporting our argumentation whereas we see $\delta^{30}\text{Si}_{\text{diatom}}$ rather as a weathering proxy at Lake Khamra overprinting the isotopic effect of bioproductivity.

In the early stage of the short core (~pre 1850 CE) we observe a slight increase of TOC, TN and OCAR (Fig. 2Fig. 5), comparable to recent decades, linked with elevated productivity (Meyers and Teranes, 2001). This overlaps with reconstructed dry and cold conditions (Stieg et al., 2024b), assumed to provide more littoral habitats at a lower lake level (discussed in diatom zone 1), which align with a lower P/B ratio, a reduced abundance of dominant *Aulacoseira* in diatom zone 1 and a simultaneously increased diatom richness (Hill numbers; Fig. 4Fig. 3).

4.4 Ecosystem alterations in Anthropogenic influence on Lake Khamra linked to atmospheric pollution

There are indications of human pollution at Lake Khamra, despite its remote location and the absence of industrial activity in its vicinity. The decline in $\delta^{13}\text{C}$ values since the 1950s (Fig. 2Fig. 5) is likely linked to the release of lighter carbon isotopes from fossil fuel combustion (Verburg, 2007), as reflected in the lake's sediments (Verburg, 2007).

A previous study (Stieg et al., 2024b) identified a marked increase in mercury concentrations in the same lake sediment samples, tripling since ~1930 CE, with fluxes rising more than fourfold since the 1990s. Mercury in the lake can originate from both natural sources, such as permafrost (Rutkowski et al., 2021) and biomass burning (Burke et al., 2010; Driscoll et al., 2013), as well as from anthropogenic sources, such as emissions (Wang et al., 2004; Streets et al., 2011). The observed increase at Lake Khamra is suggested to be at least partially related to industrial growth and associated atmospheric mercury emissions in Asia and Russia (Pacyna et al., 2016; Sundseth et al., 2017; Eckhardt et al., 2023), comparable to mercury accumulation rates observed at Lake Baikal post-1850

Formatiert: Nicht Hochgestellt/ Tiefgestellt

Formatiert: Tiefgestellt

CE (Roberts et al., 2020). Here, Besides mining activities in the vicinity of Lake Baikal, atmospheric fallout since the 1980s is also suggested to have likely contributed to rising mercury accumulation rates, in addition to mining activities in the vicinity of Lake Baikal (Roberts et al., 2020). Similarly, a rapid mercury increase since 1850 CE has been linked to atmospheric pollution at another remote boreal lake in eastern Siberia (Biskaborn et al., 2021b), suggesting that Lake Khamra is likely also influenced by anthropogenic mercury deposition. Besides the observed temperature increase due to recent global warming, we observe significant effects of human pollution at Lake Khamra despite its remote location. Mercury concentrations in the lake's sediment increase since the 1950s, with mercury fluxes (HgAR) rapidly rising since the 1990s, which has been primarily linked with human atmospheric pollution (Stieg et al., 2024b). The $\delta^{13}\text{C}$ values decline since the 1950s (Fig. 2), partly related to air pollution and the release of light carbon isotopes from burning fossil fuels.

In the same sediment samples, we observe a significant increase in the silicified chrysophyte *Mallomonas* scales (Fig. 4), an indication for lake acidification (Smol et al., 1984) and nutrient load (Munch, 1980). This recent acidification of Lake Khamra is supported by a low pH measurement of 6.07 in the surface water taken in summer 2018 (Stieg et al., 2024b), which is at the minimum range of lakes in the temperate zone with typical taiga vegetation (Pestryakova et al., 2018). Moreover, we observe a strong correlation between HgAR and the *Mallomonas* index after 1950 CE ($r = 0.92$, $p < 0.05$; Fig. A4), underlining a trend of long-distance (air) pollution. This acidification tendency is similar to that observed in another pristine lake in south Yakutia (Biskaborn et al., 2021b), where the *Mallomonas* index has also increased in the upper sediment samples.

Lake acidification is a known phenomenon (Farmer, 1990) and is often associated with the formation of S and N oxides resulting from the combustion of fossil fuels and thus, from air pollution (Moiseenko and Gashkina, 2011). Atmospheric nutrient enrichment has been reported to increase planktonic pennate diatoms such as *Tabellaria* (Rühland et al., 2015). However, at Lake Khamra we observe a decrease of *T. flocculosa* since 1970 CE, simultaneously with the increase of *D. stelligera* (Fig. 3). The high surface area to volume ratio of the eyelotelloid *Discostella* species allows it to sink less rapidly in the photic zone, enhancing light harvesting and nutrient uptake (Smol, 2023). Additionally, this species is known as opportunistic and fast-growing (Rühland et al., 2015; Saros and Anderson, 2015), making it a likely better competitor under changing lake conditions compared to *T. flocculosa*, which thrives in unpolluted lakes (Lange-Bertalot et al., 2017).

Increased abundance of *A. formosa* in oligotrophic alpine lakes in North America is linked to atmospheric N enrichment (Saros et al., 2005; Saros et al., 2010). At Lake Khamra we also observe an increase of planktonic *A. formosa* in the most recent diatom zone 5 (Fig. 3), which could be linked to atmospheric pollution, as the increase of *Asterionella*, *Fragilaria*, and *Tabellaria* taxa is documented at various locations, not restricted to North America (Rühland et al., 2015). Furthermore, atmospheric pollutants, like reactive N, can accumulate in snow deposits and enter the lake in a pulsed manner through snowmelt (Spaulding et al., 2018). This process affects lakes primarily fed by spring snowmelt (Williams et al., 2009; Spaulding et al., 2018), such as Lake Khamra.

In contrast to the recent marked increase in mercury levels and $\delta^{13}\text{C}$ depletion, $\delta^{15}\text{N}$ in Lake Khamra sediments has shown only minimal variation over the last ~220 years, fluctuating by $\pm 0.5\text{‰}$, with a slight decrease of $\sim 0.3\text{‰}$ since the 1970s (Fig. 2 Fig. 5). Human activities, such as fossil fuel combustion and fertilizer production, are relevant sources of reactive nitrogen (Nr) that contribute to the deposition of $\delta^{15}\text{N}$ -depleted nitrogen in lake sediments, typically in a range from 1–3‰ (Gruber and Galloway, 2008; Holtgrieve et al., 2011; Wolfe et al., 2013). Despite the possible influence of atmospheric pollution, no substantial $\delta^{15}\text{N}$ depletion is observed in Lake Khamra. However, not all lakes display $\delta^{15}\text{N}$ depletion, as nitrogen cycling in lakes is complex, and factors such

as nitrogen inputs, water residence time, and aquatic activity play crucial roles (Meyers and Teranes, 2001; Galloway et al., 2003; Anderson et al., 2018). For example, increased abundance of *A. formosa* in oligotrophic alpine lakes in North America has been linked to atmospheric nitrogen-enrichment deposition (Saros et al., 2005; Saros et al., 2010). At Lake Khamra, we observe only a slight increase in planktonic *A. formosa* in the most recent diatom zone 5 (Fig. 2). We suggest that this slight increase in abundance is more likely a response to climate warming and related changes in lake water mixing and thermal stability rather than nitrogen enrichment by atmospheric deposition (Sivarajah et al., 2016). This further supports the argument that Lake Khamra is primarily influenced by recent climate warming, which is altering the lake's properties, rather than by atmospheric nitrogen deposition from human sources.

1025 **5 Conclusions**

Our study of diatom assemblages and biogeochemical proxies over the last ~220 years from Lake Khamra, eastern Siberia, reveals significant distinct ecosystem changes since circa 1790 CE, likely driven by both hydroclimatic variations dynamics and human induced pollution. Our This research addresses a spatial critical gap in lake studies over shorter time periods in Yakutia.

1030 Lake Khamra's diatom assemblage is dominated by a few planktonic diatom species, primarily *Aulacoseira* taxa. At 1970 CE, we observe a drastic major shift in the diatom assemblages, characterised mainly by an increase in planktonic *D. stelligera*, while the two dominant *Aulacoseira* taxa decrease. We attribute this change to warming, a probable earlier ice-out, and a potential increase in summer thermal stratification in the recent decades. Rapidly increasing chrysophyte scales (*Mallomonas*) since the 1990s support this warming trend and a related increasing stratification of the lake. These findings are temporally consistent with similar changes observed in temperate lake ecosystems globally.

Carbon and nitrogen records proxies exhibit changes starting in the 1950s, indicating hydroclimatic influence with a delayed shift in the diatom assemblages, which we attribute primarily to rising temperatures and associated effects.

1040 At Lake Khamra, the interpretation of $\delta^{30}\text{Si}_{\text{diatom}}$ isappears not straightforward, as it is likely influenced by a combination of factors, includingincludingto reflect weathering, rather than shifts in diatom productivityassemblages, and diatom productivity. We suggest that wildfire activity in the catchment in the 1950s, along with increased precipitation and temperatures since 1970 CE, altered silica sources by—transporting isotopically light dissolved silica into the lake, which likely led to the observed decrease. Furthermore, the lower silica uptake of *D. stelligera* compared to *Aulacoseira* taxa might have further influenced this decline, overprinting the isotopic effect of bioproductivity.

1045 In addition to elevated mercury levels, determined in a previous study, human impact influence on the lake ecosystemLake Khamra is evident from $\delta^{13}\text{C}$ depletion, likely derived from fossil fuel combustion. Despite, no substantial $\delta^{15}\text{N}$ —depletion from atmospheric nitrogen deposition is observed in Lake Khamra sediments,—derived $\delta^{13}\text{C}$ depletion, pollution induced changes in diatom species and lake acidification.

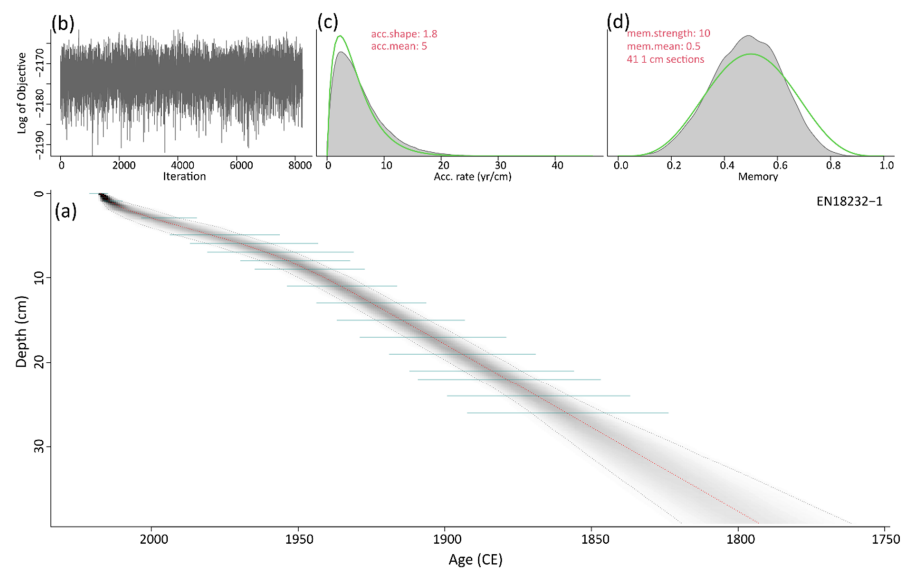
1050 These findings underline the effects of both dual impact of climate change warming and anthropogenic air pollution on remote lake ecosystems, emphasising the need for comprehensive research to mitigate these impactseffects and protect natural water resources.

Formatiert: Schriftart: Kursiv

Formatiert: Schriftart: Kursiv

Formatiert: Schriftart: Kursiv

Formatiert: Schriftart: Kursiv



1060 **Figure A1.** (a) Bayesian accumulation model based on the ^{210}Pb and ^{137}Cs dating (green lines) of the short core EN18232-1 (grey lines indicate the 2σ range; red line indicates the median). (b) Model iteration log. (c, d) Prior (green line) and posterior (grey area) distributions for accumulation rate and memory, respectively. Age–depth model was first published in Stieg et al. (2024b).

Formatiert: Links, Abstand Nach: 8 Pt., Zeilenabstand: Mehrere 1,08 ze

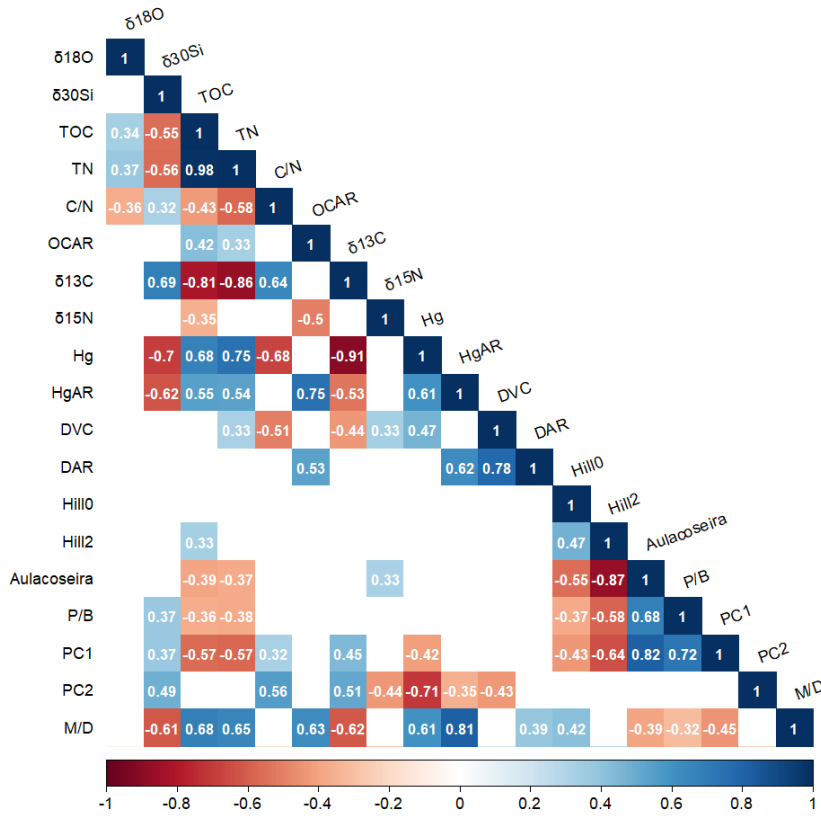


Figure A2. Pearson correlation coefficients of the short core EN18232-1: This matrix displays the Pearson correlation coefficients for selected environmental parameters. The significance threshold for correlation is set at $p < 0.05$, with non-significant correlations being blanked out.

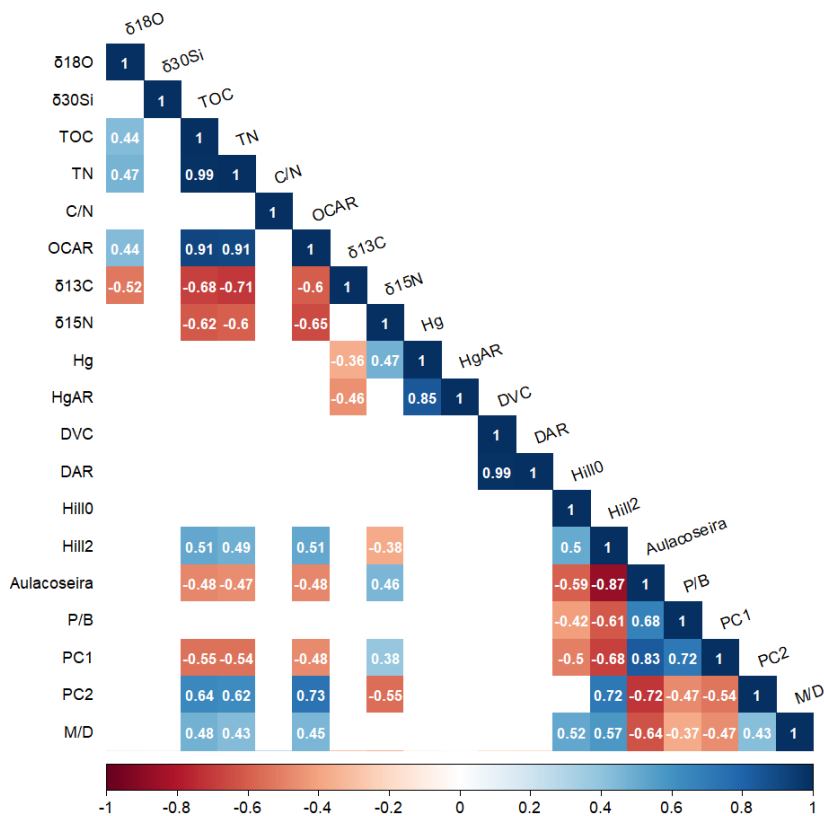


Figure A3. Pearson correlation coefficients pre-1950 CE of the short core EN18232-1: This matrix displays the Pearson correlation coefficients for selected environmental parameters from the period before 1950 CE. The significance threshold for correlation is set at $p < 0.05$, with non-significant correlations being blanked out.

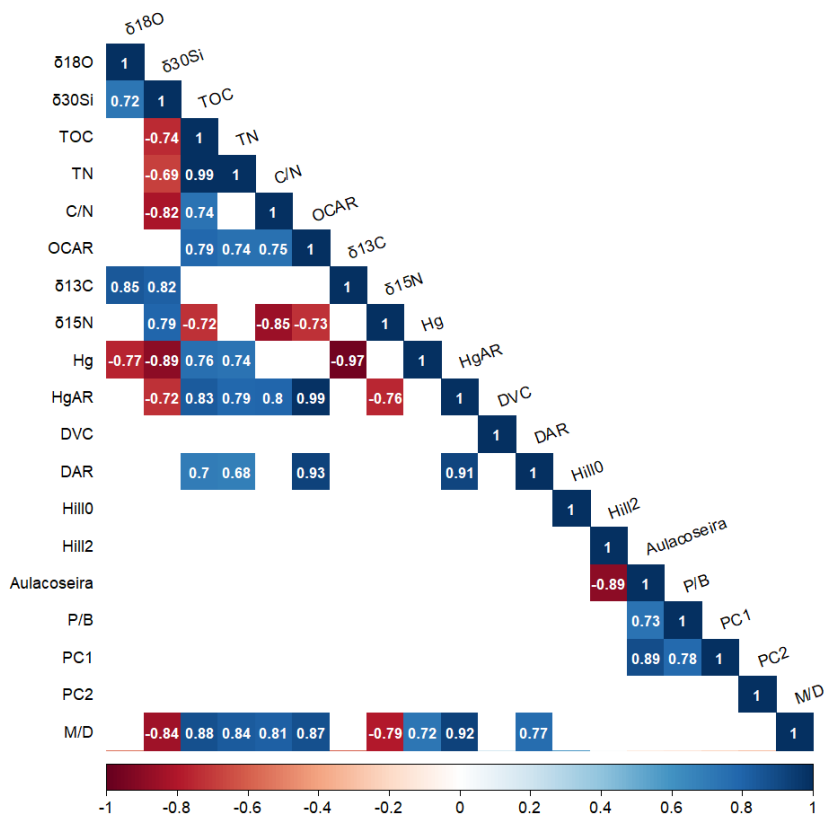


Figure A4. Pearson correlation coefficients past 1950 CE of the short core EN18232-1: This matrix displays the Pearson correlation coefficients for selected environmental parameters from the period after 1950 CE. The significance threshold for correlation is set at $p < 0.05$, with non-significant correlations being blanked out.

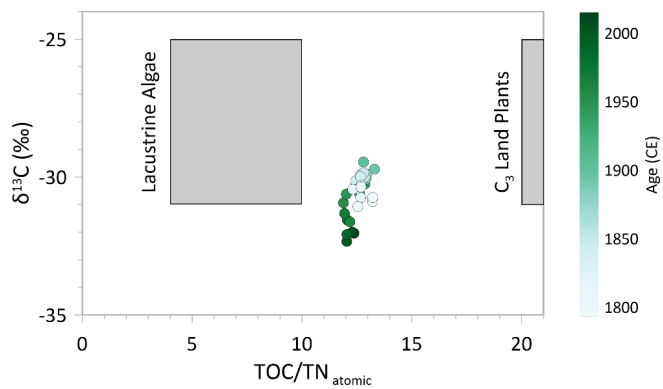


Figure A5. C/N - $\delta^{13}\text{C}$ -plot showing sediment samples of the short core EN18232-1. In general, lacustrine algae have a C/N ratio between 4 to 10, C₃ land plants have a ratio > 20 (Meyers and Teranes, 2001). Figure is based on the values given by Meyers and Teranes (2001).

Formatiert: Links, Abstand Nach: 8 Pt., Zeilenabstand: Mehrere 1,08 ze

Data availability.

Datasets used in this study are accessible via PANGAEA, including:

1. Diatom assemblage of the sediment short core EN18232-1 and corresponding indices,
<https://doi.org/10.1594/PANGAEA.971296>, Stieg et al. (dataset in review)
2. Diatom silicon isotope record of the sediment short core EN18232-1,
<https://doi.org/10.1594/PANGAEA.971278>, Stieg et al. (dataset in review)
3. Biogeochemical proxies of the sediment short core EN18232-1,
<https://doi.org/10.1594/PANGAEA.971277>, Stieg et al. (dataset in review)

Author contributions.

AS, HM, BKB and UH conceived the study. UH, BKB and LP conducted fieldwork in 2018 and 2020 and received the sediment core. AS processed and analysed the sediment samples in the lab. AS performed diatom analysis and counting, as well as statistical analysis, under the guidance of BKB. AM measured the silicon isotope samples in BHV, with the support of DWD, and helped together with HM to interpret the diatom isotopes. JS supervised the carbon and nitrogen measurements and helped to interpret the proxies. AS produced all figures and tables and wrote the manuscript. All authors commented on previous versions of the text and approved the final manuscript.

Competing interests. The authors declare that they have no conflict of interest.

Disclaimer. Colours from the scientific color maps from Crameri et al. (2020) have been used in the figures 3, 4 and 5. Maps throughout this article were created using the Free and Open Source QGIS Geographic Information System. QGIS.org, Version 3.12, 2024.

Acknowledgements. We thank the working groups of the ISOLAB Facility and the CarLa lab of the AWI in Potsdam, as well as the Stable Isotope Facility of the AWI in Bremerhaven. We would further like to thank all participants of the joint German–Russian expedition in Yakutia 2018 and 2020 for their fieldwork.

Financial support. AS is funded by AWI INSPIRES (International Science Program for Integrative Research in Earth Systems).

Formatiert: Links, Abstand Nach: 8 Pt., Zeilenabstand:
Mehrere 1,08 ze

- Alleman, L. Y., Cardinal, D., Cocquyt, C., Plisnier, P.-D., Descy, J.-P., Kimirei, I., Sinyinza, D., and André, L.: Silicon Isotopic Fractionation in Lake Tanganyika and Its Main Tributaries, *Journal of Great Lakes Research*, 31, 509-519, [https://doi.org/10.1016/S0380-1330\(05\)70280-X](https://doi.org/10.1016/S0380-1330(05)70280-X), 2005.
- AMAP: AMAP Arctic Climate Change Update 2021: Key Trends and Impacts. Arctic Monitoring and Assessment Programme (AMAP), Tromsø, Norway, viii+148pp, 978-82-7971-201-5, 2021.
- Anderson, N. J., Curtis, C. J., Whiteford, E. J., Jones, V. J., McGowan, S., Simpson, G. L., and Kaiser, J.: Regional variability in the atmospheric nitrogen deposition signal and its transfer to the sediment record in Greenland lakes, *Limnology and Oceanography*, 63, 2250-2265, 10.1002/lno.10936, 2018.
- Appleby, P. G., Nolan, P. J., Gifford, D. W., Godfrey, M. J., Oldfield, F., Anderson, N. J., and Battarbee, R. W.: ²¹⁰Pb dating by low background gamma counting, *Hydrobiologia*, 143, 21-27, 10.1007/bf00026640, 1986.
- Bahls, L. L.: The role of amateurs in modern diatom research, *Diatom Research*, 30, 209-210, 10.1080/0269249X.2014.988293, 2015.
- Barinova, S., Nevo, E., and Bragina, T.: Ecological assessment of wetland ecosystems of northern Kazakhstan on the basis of hydrochemistry and algal biodiversity, *Acta Botanica Croatica*, 70, 215-244, 10.2478/v10184-010-0020-7, 2011.
- Battarbee, R. W. and Kneen, M. J.: The use of electronically counted microspheres in absolute diatom analysis, *Limnology and Oceanography*, 27, 184-188, 10.4319/lo.1982.27.1.0184, 1982.
- Battarbee, R. W., Jones, V. J., Flower, R. J., Cameron, N. G., Bennion, H., Carvalho, L., and Juggins, S.: Diatoms, in: *Tracking Environmental Change Using Lake Sediments: Terrestrial, Algal, and Siliceous Indicators*, edited by: Smol, J. P., Birks, H. J. B., Last, W. M., Bradley, R. S., and Alverson, K., Springer Netherlands, Dordrecht, 155-202, 10.1007/0-306-47668-1_8, 978-0-306-47668-6, 2001.
- Birks, H. J. B.: Numerical methods for the analysis of diatom assemblage data, in: *The Diatoms: Applications for the Environmental and Earth Science*, edited by: Smol, J. P., and Stoermer, E. F., Cambridge University Press, Cambridge, 23-54, <https://doi.org/10.1017/CBO9780511763175>, 2010.
- Biskaborn, B. K., Herzschuh, U., Bolshiyakov, D., Savelieva, L., and Diekmann, B.: Environmental variability in northeastern Siberia during the last ~ 13,300 yr inferred from lake diatoms and sediment-geochemical parameters, *Palaeogeography, Palaeoclimatology, Palaeoecology*, 329-330, 22-36, 10.1016/j.palaeo.2012.02.003, 2012.
- Biskaborn, B. K., Bolshiyakov, D., Grigoriev, M. N., Morgenstern, A., Pestryakova, L. A., Tsimizov, L., and Dill, A.: Russian-German Cooperation: Expeditions to Siberia in 2020, *Berichte zur Polar- und Meeresforschung = Reports on polar and marine research*, Alfred Wegener Institute for Polar and Marine Research, Bremerhaven, 81, 10.48433/BzPM_0756_2021, 2021a.
- Biskaborn, B. K., Narancic, B., Stoof-Leichsenring, K. R., Pestryakova, L. A., Appleby, P. G., Piliposian, G. T., and Diekmann, B.: Effects of climate change and industrialization on Lake Bolshoe Toko, eastern Siberia, *Journal of Paleolimnology*, 65, 335-352, 10.1007/s10933-021-00175-z, 2021b.
- Biskaborn, B. K., Forster, A., Pfalz, G., Pestryakova, L. A., Stoof-Leichsenring, K., Strauss, J., Kröger, T., and Herzschuh, U.: Diatom responses and geochemical feedbacks to environmental changes at Lake Rauchuagytgyn (Far East Russian Arctic), *Biogeosciences*, 20, 1691-1712, 10.5194/bg-20-1691-2023, 2023.
- Biskaborn, B. K., Nazarova, L., Kröger, T., Pestryakova, L. A., Syrykh, L., Pfalz, G., Herzschuh, U., and Diekmann, B.: Late Quaternary Climate Reconstruction and Lead-Lag Relationships of Biotic and Sediment-Geochemical Indicators at Lake Bolshoe Toko, Siberia, *Frontiers in Earth Science*, 9, 737353, 10.3389/feart.2021.737353, 2021c.
- Biskaborn, B. K., Subetto, D. A., Savelieva, L. A., Vakhrameeva, P. S., Hansche, A., Herzschuh, U., Klemm, J., Heinecke, L., Pestryakova, L. A., Meyer, H., Kuhn, G., and Diekmann, B.: Late Quaternary vegetation and lake system dynamics in north-eastern Siberia: Implications for seasonal climate variability, *Quaternary Science Reviews*, 147, 406-421, 10.1016/j.quascirev.2015.08.014, 2016.
- Blaauw, M. and Christen, J. A.: Flexible paleoclimate age-depth models using an autoregressive gamma process, *Bayesian Analysis*, 6, 457-474, 10.1214/11-ba618, 2011.

Formatiert: Englisch (Vereinigtes Königreich)

Feldfunktion geändert

Formatiert: Englisch (Vereinigtes Königreich)

Formatiert: Englisch (Vereinigtes Königreich)

Formatiert: Schriftfarbe: Akzent 6, Englisch (Vereinigtes Königreich)

Formatiert: Englisch (Vereinigtes Königreich)

Formatiert: Englisch (Vereinigtes Königreich)

Formatiert: Englisch (Vereinigtes Königreich)

Feldfunktion geändert

170	<p>Burke, M. P., Hogue, T. S., Ferreira, M., Mendez, C. B., Navarro, B., Lopez, S., and Jay, J. A.: The Effect of Wildfire on Soil Mercury Concentrations in Southern California Watersheds, <i>Water Air Soil Pollut</i>, 212, 369-385, 10.1007/s11270-010-0351-y, 2010.</p>	<div style="border: 1px solid red; padding: 2px; font-size: 0.8em;"> Formatiert: Schriftfarbe: Akzent 6, Englisch (Vereinigtes Königreich) </div>
175	<p>Cardinal, D., Alleman, L. Y., Dehairs, F., Savoye, N., Trull, T. W., and André, L.: Relevance of silicon isotopes to Si-nutrient utilization and Si-source assessment in Antarctic waters, <i>Global Biogeochemical Cycles</i>, 19, GB2007, 10.1029/2004gb002364, 2005.</p>	<div style="border: 1px solid red; padding: 2px; font-size: 0.8em;"> Formatiert: Englisch (Vereinigtes Königreich) </div>
180	<p>Chapligin, B., Meyer, H., Friedrichsen, H., Marent, A., Sohns, E., and Hubberten, H. W.: A high-performance, safer and semi-automated approach for the $\delta^{18}\text{O}$ analysis of diatom silica and new methods for removing exchangeable oxygen, <i>Rapid Commun Mass Spectrom</i>, 24, 2655-2664, 10.1002/rcm.4689, 2010.</p>	<div style="border: 1px solid red; padding: 2px; font-size: 0.8em;"> Formatiert: Englisch (Vereinigtes Königreich) </div>
185	<p>Chelnokova, S. M., Chikina, I. D., and Radchenko, S. A. Geologic map of Yakutia P-48,49, 1 : 1000000, VSEGEI, Leningrad: http://www.geokniga.org/sites/geokniga/, last access: 11. November 2022.</p>	<div style="border: 1px solid red; padding: 2px; font-size: 0.8em;"> Feldfunktion geändert </div>
190	<p>Chen, J., Li, J., Tian, S., Kalugin, I., Darin, A., and Xu, S.: Silicon isotope composition of diatoms as a paleoenvironmental proxy in Lake Huguangyan, South China, <i>Journal of Asian Earth Sciences</i>, 45, 268-274, 10.1016/j.jseaes.2011.11.010, 2012.</p>	<div style="border: 1px solid red; padding: 2px; font-size: 0.8em;"> Formatiert: Englisch (Vereinigtes Königreich) </div>
195	<p>Cherapanova, M. V., Snyder, J. A., and Brigham-Grette, J.: Diatom stratigraphy of the last 250 ka at Lake El'gygytgyn, northeast Siberia, <i>Journal of Paleolimnology</i>, 37, 155-162, 10.1007/s10933-006-9019-4, 2006.</p>	<div style="border: 1px solid red; padding: 2px; font-size: 0.8em;"> Formatiert: Englisch (Vereinigtes Königreich) </div>
200	<p>Clayton, R. N. and Mayeda, T. K.: The use of bromine pentafluoride in the extraction of oxygen from oxides and silicates for isotopic analysis, <i>Geochim Cosmochim Acta</i>, 27, 43-52, 10.1016/0016-7037(63)90071-1, 1963.</p>	<div style="border: 1px solid red; padding: 2px; font-size: 0.8em;"> Formatiert: Englisch (Vereinigtes Königreich), Durchgestrichen </div>
205	<p>Coddington, O., Lean, J. L., Lindholm, D., Pilewski, P., Snow, M., and Program, N. C.: NOAA Climate Data Record (CDR) of Total Solar Irradiance (TSI), NRTSI Version 2 [dataset], 10.7289/V55B00C1 2015.</p>	<div style="border: 1px solid red; padding: 2px; font-size: 0.8em;"> Formatiert: Englisch (Vereinigtes Königreich) </div>
210	<p>Cramer, F., Shephard, G. E., and Heron, P. J.: The misuse of colour in science communication, <i>Nat Commun</i>, 11, 5444, 10.1038/s41467-020-19160-7, 2020.</p>	<div style="border: 1px solid red; padding: 2px; font-size: 0.8em;"> Formatiert: Englisch (Vereinigtes Königreich) </div>
215	<p>Crutzen, P. J. and Stoermer, E. F.: The "Anthropocene", <i>Global Change Newsletters</i>, 41, 17-18, 0284-5865, 2000.</p>	<div style="border: 1px solid red; padding: 2px; font-size: 0.8em;"> Formatiert: Englisch (Vereinigtes Königreich) </div>
	<p>De La Rocha, C. L.: Opal-based isotopic proxies of paleoenvironmental conditions, <i>Global Biogeochemical Cycles</i>, 20, GB4509, 10.1029/2005gb002664, 2006.</p>	<div style="border: 1px solid red; padding: 2px; font-size: 0.8em;"> Formatiert: Schriftfarbe: Akzent 6, Englisch (Vereinigtes Königreich) </div>
	<p>De La Rocha, C. L., Brzezinski, M. A., and DeNiro, M. J.: Fractionation of silicon isotopes by marine diatoms during biogenic silica formation, <i>Geochim Cosmochim Acta</i>, 61, 5051-5056, Doi 10.1016/S0016-7037(97)00300-1, 1997.</p>	<div style="border: 1px solid red; padding: 2px; font-size: 0.8em;"> Formatiert: Englisch (Vereinigtes Königreich) </div>
	<p>De la Rocha, C. L., Brzezinski, M. A., and DeNiro, M. J.: A first look at the distribution of the stable isotopes of silicon in natural waters, <i>Geochim Cosmochim Acta</i>, 64, 2467-2477, 10.1016/S0016-7037(00)00373-2, 2000.</p>	<div style="border: 1px solid red; padding: 2px; font-size: 0.8em;"> Formatiert: Schriftfarbe: Akzent 6, Englisch (Vereinigtes Königreich) </div>
	<p>De La Rocha, C. L., Brzezinski, M. A., DeNiro, M. J., and Shemesh, A.: Silicon-isotope composition of diatoms as an indicator of past oceanic change, <i>Nature</i>, 395, 680-683, Doi 10.1038/27174, 1998.</p>	<div style="border: 1px solid red; padding: 2px; font-size: 0.8em;"> Formatiert: Englisch (Vereinigtes Königreich) </div>
	<p>Dixon, W. J.: Processing Data for Outliers, <i>Biometrics</i>, 9, 74 - 89, 10.2307/3001634, 1953.</p>	<div style="border: 1px solid red; padding: 2px; font-size: 0.8em;"> Formatiert: Englisch (Vereinigtes Königreich) </div>
	<p>Douglas, M. S. V. and Smol, J. P.: Freshwater diatoms as indicators of environmental change in the High Arctic, in: <i>The diatoms: applications for the environmental and earth sciences</i>, edited by: Smol, J. P., and Stoermer, E. F., Cambridge University Press, Cambridge, 249-266, 9780521509961, 2010.</p>	<div style="border: 1px solid red; padding: 2px; font-size: 0.8em;"> Formatiert: Schriftfarbe: Akzent 6, Englisch (Vereinigtes Königreich) </div>
	<p>Driscoll, C. T., Mason, R. P., Chan, H. M., Jacob, D. J., and Pirrone, N.: Mercury as a Global Pollutant: Sources, Pathways, and Effects, <i>Environmental Science & Technology</i>, 47, 4967-4983, 10.1021/es305071v, 2013.</p>	<div style="border: 1px solid red; padding: 2px; font-size: 0.8em;"> Formatiert: Englisch (Vereinigtes Königreich) </div>
	<p>Eckhardt, S., Pissot, I., Evangelidou, N., Zwaafink, C. G., Plach, A., McConnell, J. R., Sigl, M., Ruppel, M., Zdanowicz, C., Lim, S., Chellman, N., Opel, T., Meyer, H., Steffensen, J. P., Schwikowski, M., and Stohl, A.: Revised historical Northern Hemisphere black carbon emissions based on inverse modeling of ice core records, <i>Nat Commun</i>, 14, 271, 10.1038/s41467-022-35660-0, 2023.</p>	<div style="border: 1px solid red; padding: 2px; font-size: 0.8em;"> Formatiert: Schriftfarbe: Akzent 6, Englisch (Vereinigtes Königreich) </div>
	<p>Farmer, A. M.: The effects of lake acidification on aquatic macrophytes – a review, <i>Environ Pollut</i>, 65, 219-240, 10.1016/0269-7491(90)90085-q, 1990.</p>	<div style="border: 1px solid red; padding: 2px; font-size: 0.8em;"> Formatiert: Englisch (Vereinigtes Königreich), Durchgestrichen </div>
	<p>Favot, E. J., Rühland, K. M., Paterson, A. M., and Smol, J. P.: Sediment records from Lake Nipissing (ON, Canada) register a lake-wide multi-trophic response to climate change and reveal its possible role for</p>	<div style="border: 1px solid red; padding: 2px; font-size: 0.8em;"> Formatiert: Englisch (Vereinigtes Königreich) </div> <div style="border: 1px solid red; padding: 2px; font-size: 0.8em;"> Formatiert: Schriftfarbe: Akzent 6, Englisch (Vereinigtes Königreich) </div>

increased cyanobacterial blooms, *Journal of Great Lakes Research*, 50, 10.1016/j.jglr.2023.102268, 2024.

220 Fedorov, A., Vasilyev, N., Torgovkin, Y., Shestakova, A., Varlamov, S., Zheleznyak, M., Shepelev, V., Konstantinov, P., Kalinicheva, S., Basharin, N., Makarov, V., Ugarov, I., Efremov, P., Argunov, R., Egorova, L., Samsonova, V., Shepelev, A., Vasiliev, A., Ivanova, R., Galanin, A., Lytkin, V., Kuzmin, G., and Kunitsky, V.: Permafrost-Landscape Map of the Republic of Sakha (Yakutia) on a Scale 1:1,500,000, *Geosciences*, 8, 465 - 481, 10.3390/geosciences8120465, 2018.

225 Firsova, A. D., Chebykin, E. P., Kopyrina, L. I., Rodionova, E. V., Chensky, D. A., Gubin, N. A., Panov, V. S., Pogodaeva, T. V., Bukin, Y. S., Suturin, A. N., and Likhoshway, Y. V.: Post-glacial diatom and geochemical records of ecological status and water level changes of Lake Vorota, Western Beringia, *Journal of Paleolimnology*, 66, 407-437, 10.1007/s10933-021-00214-9, 2021.

230 Frings, P. J., Panizzo, V. N., Sutton, J. N., and Ehlert, C.: Diatom silicon isotope ratios in Quaternary research: Where do we stand?, *Quaternary Science Reviews*, 344, 10.1016/j.quascirev.2024.108966, 2024.

Frings, P. J., Clymans, W., Fontorbe, G., De La Rocha, C. L., and Conley, D. J.: The continental Si cycle and its impact on the ocean Si isotope budget, *Chemical Geology*, 425, 12-36, 10.1016/j.chemgeo.2016.01.020, 2016.

235 Galloway, J. N., Aber, J. D., Erisman, J. W., Seitzinger, S. P., Howarth, R. W., Cowling, E. B., and Cosby, B. J.: The nitrogen cascade, *Bioscience*, 53, 341-356, Doi 10.1641/0006-3568(2003)053[0341:Tnc]2.0.Co;2, 2003.

Geng, R., Andreev, A., Kruse, S., Heim, B., van Geffen, F., Pestryakova, L., Zakharov, E., Troeva, E., Shevtsova, I., Li, F., Zhao, Y., and Herzsuh, U.: Modern Pollen Assemblages From Lake Sediments and Soil in East Siberia and Relative Pollen Productivity Estimates for Major Taxa, *Frontiers in Ecology and Evolution*, 10, 837857, 10.3389/fevo.2022.837857, 2022.

240 Gibson, C. E., Anderson, N. J., and Haworth, E. Y.: *Aulacoseira subarctica*: taxonomy, physiology, ecology and palaeoecology, *European Journal of Phycology*, 38, 83-101, 10.1080/0967026031000094102, 2003.

245 Ginn, B. K., Rate, M., Cumming, B. F., and Smol, J. P.: Ecological distribution of scaled-chrysophyte assemblages from the sediments of 54 lakes in Nova Scotia and southern New Brunswick, Canada, *Journal of Paleolimnology*, 43, 293-308, 10.1007/s10933-009-9332-9, 2010.

Glückler, R., Herzsuh, U., Kruse, S., Andreev, A., Vyse, S. A., Winkler, B., Biskaborn, B. K., Pestryakova, L., and Dietze, E.: Wildfire history of the boreal forest of south-western Yakutia (Siberia) over the last two millennia documented by a lake-sediment charcoal record, *Biogeosciences*, 18, 4185-4209, 10.5194/bg-18-4185-2021, 2021.

250 Gorokhov, A. N. and Fedorov, A. N.: Current Trends in Climate Change in Yakutia, *Geography and Natural Resources*, 39, 153-161, 10.1134/s1875372818020087, 2018.

Grimm, E. C.: Coniss - a Fortran-77 Program for Stratigraphically Constrained Cluster-Analysis by the Method of Incremental Sum of Squares, *Comput Geosci*, 13, 13-35, 10.1016/0098-3004(87)90022-7, 1987.

255 Gruber, N. and Galloway, J. N.: An Earth-system perspective of the global nitrogen cycle, *Nature*, 451, 293-296, 10.1038/nature06592, 2008.

Guiry, M. D. and Guiry, G. M. *AlgaeBase*. World-wide electronic publication, National University of Ireland, Galway.: <https://www.algaebase.org>, last access: 1. August 2024.

260 Håkansson, H. and Kling, H.: A light and electron microscope study of previously described and new *Stephanodiscus* species (bacillariophyceae) from central and northern Canadian lakes, with ecological notes on the species, *Diatom Research*, 4, 269-288, 10.1080/0269249X.1989.9705076, 1989.

265 Hampton, S. E., Gray, D. K., Izmet's'eva, L. R., Moore, M. V., and Ozersky, T.: The rise and fall of plankton: long-term changes in the vertical distribution of algae and grazers in Lake Baikal, Siberia, *PLoS One*, 9, e88920, 10.1371/journal.pone.0088920, 2014.

Hampton, S. E., Izmet's'eva, L. R., Moore, M. V., Katz, S. L., Dennis, B., and Silow, E. A.: Sixty years of environmental change in the world's largest freshwater lake – Lake Baikal, Siberia, *Global Change Biology*, 14, 1947-1958, 10.1111/j.1365-2486.2008.01616.x, 2008.

Formatiert: Englisch (Vereinigtes Königreich)

Formatiert: Schriftfarbe: Akzent 6, Englisch (Vereinigtes Königreich)

Formatiert: Englisch (Vereinigtes Königreich)

Formatiert: Schriftfarbe: Akzent 6, Englisch (Vereinigtes Königreich)

Formatiert: Englisch (Vereinigtes Königreich)

Formatiert: Schriftfarbe: Akzent 6, Englisch (Vereinigtes Königreich)

Formatiert: Englisch (Vereinigtes Königreich)

Feldfunktion geändert

Formatiert: Englisch (Vereinigtes Königreich)

Formatiert: Englisch (Vereinigtes Königreich)

Formatiert: Schriftfarbe: Akzent 6, Englisch (Vereinigtes Königreich)

Hampton, S. E., McGowan, S., Ozersky, T., Virdis, S. G. P., Vu, T. T., Spanbauer, T. L., Kraemer, B. M., Swann, G., Mackay, A. W., Powers, S. M., Meyer, M. F., Labou, S. G., O'Reilly, C. M., DiCarlo, M., Galloway, A. W. E., and Fritz, S. C.: Recent ecological change in ancient lakes, *Limnology and Oceanography*, 63, 2277-2304, 10.1002/lno.10938, 2018.

Hampton, S. E., Galloway, A. W., Powers, S. M., Ozersky, T., Woo, K. H., Batt, R. D., Labou, S. G., O'Reilly, C. M., Sharma, S., Lottig, N. R., Stanley, E. H., North, R. L., Stockwell, J. D., Adrian, R., Weyhenmeyer, G. A., Arvola, L., Baulch, H. M., Bertani, I., Bowman, L. L., Jr., Carey, C. C., Catalan, J., Colom-Montero, W., Domine, L. M., Felip, M., Granados, I., Gries, C., Grossart, H. P., Haberman, J., Haldna, M., Hayden, B., Higgins, S. N., Jolley, J. C., Kahilainen, K. K., Kaup, E., Kehoe, M. J., MacIntyre, S., Mackay, A. W., Mariash, H. L., McKay, R. M., Nixdorf, B., Noges, P., Noges, T., Palmer, M., Pierson, D. C., Post, D. M., Pruett, M. J., Rautio, M., Read, J. S., Roberts, S. L., Rucker, J., Sadro, S., Silow, E. A., Smith, D. E., Sterner, R. W., Swann, G. E., Timofeyev, M. A., Toro, M., Twiss, M. R., Vogt, R. J., Watson, S. B., Whiteford, E. J., and Xenopoulos, M. A.: Ecology under lake ice, *Ecol Lett*, 20, 98-111, 10.1111/ele.12699, 2017.

~~Heudre, D., Wetzel, C. E., Lange-Bertalot, H., Van de Vijver, B., Moreau, L., and Ector, L.: A review of Tabellaria species from freshwater environments in Europe, *Fottea*, 21, 180-205, 10.5507/fot.2021.005, 2021.~~

Hofmann, G., Lange-Bertalot, H., and Werum, M.: Diatomeen im Süßwasser-Benthos von Mitteleuropa: Bestimmungsflora Kieselalgen für die ökologische Praxis; über 700 der häufigsten Arten und ihre Ökologie, A.R.G. Gantner Verlag K.G., 908 pp., 9783906166926, 2011.

Holtgrieve, G. W., Schindler, D. E., Hobbs, W. O., Leavitt, P. R., Ward, E. J., Bunting, L., Chen, G., Finney, B. P., Gregory-Eaves, I., Holmgren, S., Lisac, M. J., Lisi, P. J., Nydick, K., Rogers, L. A., Saros, J. E., Selbie, D. T., Shapley, M. D., Walsh, P. B., and Wolfe, A. P.: A coherent signature of anthropogenic nitrogen deposition to remote watersheds of the Northern Hemisphere, *Science*, 334, 1545-1548, 10.1126/science.1212267, 2011.

Horn, H., Paul, L., Horn, W., and Petzoldt, T.: Long-term trends in the diatom composition of the spring bloom of a German reservoir: is *Aulacoseira subarctica* favoured by warm winters?, *Freshwater Biology*, 56, 2483-2499, 10.1111/j.1365-2427.2011.02674.x, 2011.

Huang, S., Zhang, K., Lin, Q., Liu, J., and Shen, J.: Abrupt ecological shifts of lakes during the Anthropocene, *Earth-Science Reviews*, 227, 103981, 10.1016/j.earscirev.2022.103981, 2022.

JCS, I. C. o. S. International Commission on Stratigraphy. Subcommittee on Quaternary Stratigraphy. Working Group on the 'Anthropocene': <https://quaternary.stratigraphy.org/working-groups/anthropocene>, last access: 18. November 2024.

Izmet'eva, L. R., Moore, M. V., Hampton, S. E., Ferwerda, C. J., Gray, D. K., Woo, K. H., Pislegina, H. V., Krashchuk, L. S., Shimaraeva, S. V., and Silow, E. A.: Lake-wide physical and biological trends associated with warming in Lake Baikal, *Journal of Great Lakes Research*, 42, 6-17, 10.1016/j.jglr.2015.11.006, 2016.

~~Jasinski, J. P., Warner, B. G., Andreev, A. A., Aravena, R., Gilbert, S. E., Zeeb, B. A., Smol, J. P., and Velichko, A. A.: Holocene environmental history of a peatland in the Lena River valley, Siberia, *Canadian Journal of Earth Sciences*, 35, 637-648, 10.1139/e98-015, 1998.~~

Jiang, S., Liu, X., Sun, J., Yuan, L., Sun, L., and Wang, Y.: A multi-proxy sediment record of late Holocene and recent climate change from a lake near Ny-Ålesund, Svalbard, *Boreas*, 40, 468-480, 10.1111/j.1502-3885.2010.00198.x, 2011.

Jones, V. J., Rose, N. L., Self, A. E., Solovieva, N., and Yang, H.: Evidence of global pollution and recent environmental change in Kamchatka, Russia, *Global and Planetary Change*, 134, 82-90, 10.1016/j.gloplacha.2015.02.005, 2015.

Juggins, S. Juggins, S.: Rioja: Analysis of Quaternary Science Data, R package: <https://cran.r-project.org/package=rioja>, last access: 25. February 2024.

Kahlert, M., Rühland, K. M., Lavoie, I., Keck, F., Saulnier-Talbot, E., Bogan, D., Brua, R. B., Campeau, S., Christoffersen, K. S., Culp, J. M., Karjalainen, S. M., Lento, J., Schneider, S. C., Shaftel, R., and Smol, J. P.: Biodiversity patterns of Arctic diatom assemblages in lakes and streams: Current reference conditions and historical context for biomonitoring, *Freshwater Biology*, 67, 116-140, 10.1111/fwb.13490, 2020.

Formatiert: Englisch (Vereinigtes Königreich), Durchgestrichen

Formatiert: Schriftfarbe: Akzent 6, Englisch (Vereinigtes Königreich)

Formatiert: Englisch (Vereinigtes Königreich)

Formatiert: Schriftfarbe: Akzent 6, Englisch (Vereinigtes Königreich)

Formatiert: Schriftfarbe: Akzent 6

Formatiert: Schriftfarbe: Akzent 6, Englisch (Vereinigtes Königreich)

Formatiert: Englisch (Vereinigtes Königreich), Durchgestrichen

Formatiert: Englisch (Vereinigtes Königreich)

Feldfunktion geändert

Formatiert: Englisch (Vereinigtes Königreich)

Formatiert: Englisch (Vereinigtes Königreich)

Keeling, C. D.: The Suess effect: ^{13}C - ^{14}C interrelations, *Environment International*, 2, 229-300, 10.1016/0160-4120(79)90005-9, 1979.

Kilham, P., Kilham, S. S., and Hecky, R. E.: Hypothesized resource relationships among African planktonic diatoms, *Limnology and Oceanography*, 31, 1169-1181, 10.4319/lo.1986.31.6.1169, 1986.

Kilham, S. S., Theriot, E. C., and Fritz, S. C.: Linking planktonic diatoms and climate change in the large lakes of the Yellowstone ecosystem using resource theory, *Limnology and Oceanography*, 41, 1052-1062, DOI 10.4319/lo.1996.41.5.1052, 1996.

Kirillina, K., Shvetsov, E. G., Protopopova, V. V., Thiesmeyer, L., and Yan, W.: Consideration of anthropogenic factors in boreal forest fire regime changes during rapid socio-economic development: case study of forestry districts with increasing burnt area in the Sakha Republic, Russia, *Environmental Research Letters*, 15, 035009, 10.1088/1748-9326/ab6c6e, 2020.

Klein Tank, A. M. G., Wijngaard, J. B., Können, G. P., Böhm, R., Demarée, G., Gocheva, A., Mileta, M., Pashiardis, S., Hejkrlik, L., Kern-Hansen, C., Heino, R., Bessemoulin, P., Müller-Westermeier, G., Tzanakou, M., Szalai, S., Pálsdóttir, T., Fitzgerald, D., Rubin, S., Capaldo, M., Maugeri, M., Leitass, A., Bukantis, A., Aberfeld, R., van Engelen, A. F. V., Forland, E., Miletus, M., Coelho, F., Mares, C., Razuvaev, V., Nieplová, E., Cegnar, T., Antonio López, J., Dahlström, B., Moberg, A., Kirchhofer, W., Ceylan, A., Pachaliuk, O., Alexander, L. V., and Petrovic, P.: Daily dataset of 20th-century surface air temperature and precipitation series for the European Climate Assessment, *International Journal of Climatology*, 22, 1441-1453, 10.1002/joc.773, 2002.

Komarenko, L. E. and Vasilyeva, I. I.: *Presnovodnyye diatomovye i senezelenye vodorosli vodoemov Yakutii*. [Freshwater diatoms and blue-green algae of water bodies of Yakutia] [in Russian], 96 figs., Moscow: Akad. Nauk SSSR, Sibirskoe Otdel., Yakutskii Filial, Inst. Biol., Izdatel. Nauka., [1]-423 pp., 1975.

Kostrova, S. S., Biskaborn, B. K., Pestryakova, L. A., Fernandoy, F., Lenz, M. M., and Meyer, H.: Climate and environmental changes of the Lateglacial transition and Holocene in northeastern Siberia: Evidence from diatom oxygen isotopes and assemblage composition at Lake Emanda, *Quaternary Science Reviews*, 259, 106905, 10.1016/j.quascirev.2021.106905, 2021.

Krammer, K. and Lange-Bertalot, H.: *Bacillariophyceae*, 4. Teil: Achnantheaceae, Kritische Ergänzungen zu *Navicula* (Lineolatae) und *Gomphonema*, Gesamtliteraturverzeichnis Teil 1 - 4, Süßwasserflora von Mitteleuropa, Band 2/4, Gustav Fischer Verlag, Stuttgart, Jena, 3437306642, 1991.

Krammer, K. and Lange-Bertalot, H.: *Bacillariophyceae*, 1. Teil: Naviculaceae, Süßwasserflora von Mitteleuropa, Band 2/1, Gustav Fischer Verlag, Jena, 3437353969, 1997a.

Krammer, K. and Lange-Bertalot, H.: *Bacillariophyceae*, 2. Teil: Bacillariaceae, Epithemiaceae, Surirellaceae, Süßwasserflora von Mitteleuropa, Band 2/2, Gustav Fischer Verlag, Jena, 3437353888, 1997b.

Krammer, K., Lange-Bertalot, H., Håkansson, H., and Nörpel, M.: *Bacillariophyceae*, 3. Teil: Centrales, Fragilariaceae, Eunotiaceae, Süßwasserflora von Mitteleuropa, Band 2/3, Gustav Fischer Verlag, Stuttgart, Jena, 3437305417, 1991.

Kruse, S., Bolshiyarov, D., Grigoriev, M. N., Morgenstern, A., Pestryakova, L., Tsimov, L., and Udke, A.: Russian-German Cooperation: Expeditions to Siberia in 2018, Alfred Wegener Institute for Polar and Marine Research, Bremerhaven, 263, https://doi.org/10.2312/BzPM_0734_2019, 2019.

Laing, T. E. and Smol, J. P.: Late Holocene environmental changes inferred from diatoms in a lake on the western Taimyr Peninsula, northern Russia, *Journal of Paleolimnology*, 30, 231-247, 10.1023/A:1025561905506, 2003.

Lange-Bertalot, H., Hofmann, G., Werum, M., and Cantonati, M.: *Freshwater benthic diatoms of Central Europe: over 800 common species used in ecological assessment*, Koeltz Botanical Books, Schmitt-Oberrufenberg/Germany, 942 pp., 978-3-946583-06-6, 2017.

Leng, M. J. and Barker, P. A.: A review of the oxygen isotope composition of lacustrine diatom silica for palaeoclimate reconstruction, *Earth-Science Reviews*, 75, 5-27, 10.1016/j.earscirev.2005.10.001, 2006.

Formatiert: Schriftfarbe: Akzent 6, Englisch (Vereinigtes Königreich)

Formatiert: Englisch (Vereinigtes Königreich)

Formatiert: Schriftfarbe: Akzent 6, Englisch (Vereinigtes Königreich)

Formatiert: Englisch (Vereinigtes Königreich)

Formatiert: Englisch (Vereinigtes Königreich)

Formatiert: Englisch (Vereinigtes Königreich)

Formatiert: Englisch (Vereinigtes Königreich)

Feldfunktion geändert

Formatiert: Englisch (Vereinigtes Königreich)

Formatiert: Englisch (Vereinigtes Königreich)

Formatiert: Englisch (Vereinigtes Königreich), Durchgestrichen

Formatiert: Englisch (Vereinigtes Königreich)

Leng, M. J. and Sloane, H. J.: Combined oxygen and silicon isotope analysis of biogenic silica, *Journal of Quaternary Science*, 23, 313-319, 10.1002/jqs.1177, 2008.

375 Leng, M. J., Swann, G. E. A., Hodson, M. J., Tyler, J. J., Patwardhan, S. V., and Sloane, H. J.: The Potential use of Silicon Isotope Composition of Biogenic Silica as a Proxy for Environmental Change, *Silicon*, 1, 65-77, 10.1007/s12633-009-9014-2, 2009.

380 Mackay, A. W., Ryves, D. B., Morley, D. W., Jewson, D. H., and Rioual, P.: Assessing the vulnerability of endemic diatom species in Lake Baikal to predicted future climate change: a multivariate approach, *Global Change Biology*, 12, 2297-2315, 10.1111/j.1365-2486.2006.01270.x, 2006.

Mackay, A. W., Felde, V. A., Morley, D. W., Piotrowska, N., Rioual, P., Seddon, A. W. R., and Swann, G. E. A.: Long-term trends in diatom diversity and palaeoproductivity: a 16 000-year multidecadal record from Lake Baikal, southern Siberia, *Clim Past*, 18, 363-380, 10.5194/cp-18-363-2022, 2022.

385 Maier, E., Chaplign, B., Abelmann, A., Gersonde, R., Esper, O., Ren, J., Friedrichsen, H., Meyer, H., and Tiedemann, R.: Combined oxygen and silicon isotope analysis of diatom silica from a deglacial subarctic Pacific record, *Journal of Quaternary Science*, 28, 571-581, 10.1002/jqs.2649, 2013.

Makarova, I. V.: *Diatomovye vodorosli Rossii i sopredel'nyh stran: iskopaemye i sovremennye. (The diatoms of Russia and adjacent countries: fossil and recent.)* Vol. II, issue 3. , St. Petersburg: St. Petersburg State University Publishers, 2002.

390 Messenger, M. L., Lehner, B., Grill, G., Nedeva, I., and Schmitt, O.: Estimating the volume and age of water stored in global lakes using a geo-statistical approach, *Nat Commun*, 7, 13603, 10.1038/ncomms13603, 2016.

Meyers, P. A.: Organic Geochemical Proxies, in: *Encyclopedia of Paleoclimatology and Ancient Environments. Encyclopedia of Earth Sciences Series.*, edited by: Gornitz, V., Springer, Dordrecht, 659-663, https://doi.org/10.1007/978-1-4020-4411-3_160, 978-1-4020-4551-6, 2009.

395 Meyers, P. A. and Teranes, J. L.: Sediment Organic Matter, in: *Tracking environmental change using lake sediments. Volume 2: Physical and Geochemical Methods.*, edited by: Last, W. M., and Smol, J. P., Kluwer Academic Publishers, The Netherlands, 239-269, 1402006284, 2001.

Michelutti, N., Cooke, C. A., Hobbs, W. O., and Smol, J. P.: Climate-driven changes in lakes from the Peruvian Andes, *Journal of Paleolimnology*, 54, 153-160, 10.1007/s10933-015-9843-5, 2015.

Miesner, T., Herzschuh, U., Pestryakova, L. A., Wieczorek, M., Zakharov, E. S., Kolmogorov, A. I., Davydova, P. V., and Kruse, S.: Forest structure and individual tree inventories of northeastern Siberia along climatic gradients, *Earth Syst. Sci. Data*, 14, 5695-5716, 10.5194/essd-14-5695-2022, 2022.

400 Moiseenko, T. I. and Gashkina, N. A.: Zonal features of lake acidification, *Water Resources*, 38, 47-62, 10.1134/S0097807811010076, 2011.

Moiseeva, A. I. and Nikolaev, V. A.: *Diatomovye vodorosli SSSR. Iskopaemye i sovremennye. (The diatoms of the USSR. Fossil and recent.)* Vol. II-2. , Leningrad: Nauka, 1992.

405 Moore, M. V., Hampton, S. E., Izmet'seva, L. R., Silow, E. A., Peshkova, E. V., and Pavlov, B. K.: Climate Change and the World's "Sacred Sea"—Lake Baikal, Siberia, *BioScience*, 59, 405-417, 10.1525/bio.2009.59.5.8, 2009.

410 Moos, M. T., Laird, K. R., and Cumming, B. F.: Climate-related eutrophication of a small boreal lake in northwestern Ontario: a palaeolimnological perspective, *Holocene*, 19, 359-367, 10.1177/0959683608101387, 2009.

Morley, D. W., Leng, M. J., Mackay, A. W., Sloane, H. J., Rioual, P., and Battarbee, R. W.: Cleaning of lake sediment samples for diatom oxygen isotope analysis, *Journal of Paleolimnology*, 31, 391-401, 10.1023/B:JOPL.0000021854.70714.6b, 2004.

415 Munch, C. S.: Fossil diatoms and scales of Chrysophyceae in the recent history of Hall Lake, Washington, *Freshwater Biology*, 10, 61-66, 10.1111/j.1365-2427.1980.tb01180.x, 1980.

Mushet, G. R., Laird, K. R., Das, B., Hesjedal, B., Leavitt, P. R., Scott, K. A., Simpson, G. L., Wissel, B., Wolfe, J. D., and Cumming, B. F.: Regional climate changes drive increased scaled-chrysophyte abundance in lakes downwind of Athabasca Oil Sands nitrogen emissions, *Journal of Paleolimnology*, 58, 419-435, 10.1007/s10933-017-9987-6, 2017.

420 Narancic, B., Pienitz, R., Chaplign, B., Meyer, H., Francus, P., and Guilbault, J. P.: Postglacial environmental succession of Nettiing Lake (Baffin Island, Canadian Arctic) inferred from

Formatiert: Schriftfarbe: Akzent 6, Englisch (Vereinigtes Königreich)

Formatiert: Englisch (Vereinigtes Königreich)

Formatiert: Schriftfarbe: Akzent 6, Englisch (Vereinigtes Königreich)

Formatiert: Englisch (Vereinigtes Königreich)

Feldfunktion geändert

Formatiert: Englisch (Vereinigtes Königreich)

Formatiert: Englisch (Vereinigtes Königreich)

Formatiert: Englisch (Vereinigtes Königreich), Durchgestrichen

Formatiert: Schriftfarbe: Akzent 6, Englisch (Vereinigtes Königreich)

Formatiert: Englisch (Vereinigtes Königreich)

Formatiert: Englisch (Vereinigtes Königreich), Durchgestrichen

Formatiert: Englisch (Vereinigtes Königreich)

Formatiert: Englisch (Vereinigtes Königreich), Durchgestrichen

Formatiert: Schriftfarbe: Akzent 6, Englisch (Vereinigtes Königreich)

Formatiert: Englisch (Vereinigtes Königreich), Durchgestrichen

biogeochemical and microfossil proxies, *Quaternary Science Reviews*, 147, 391–405, 10.1016/j.quascirev.2015.12.022, 2016.

O'Reilly, C. M., Sharma, S., Gray, D. K., Hampton, S. E., Read, J. S., Rowley, R. J., Schneider, P., Lenters, J. D., McIntyre, P. B., Kraemer, B. M., Weyhenmeyer, G. A., Straile, D., Dong, B., Adrian, R., Allan, M. G., Anneville, O., Arvola, L., Austin, J., Bailey, J. L., Baron, J. S., Brookes, J. D., de Eyto, E., Dokulil, M. T., Hamilton, D. P., Havens, K., Hetherington, A. L., Higgins, S. N., Hook, S., Izmet'eva, L. R., Joehnk, K. D., Kangur, K., Kasprzak, P., Kumagai, M., Kuusisto, E., Leshkevich, G., Livingstone, D. M., MacIntyre, S., May, L., Melack, J. M., Mueller-Navarra, D. C., Naumenko, M., Noges, P., Noges, T., North, R. P., Plisnier, P. D., Rigosi, A., Rimmer, A., Rogora, M., Rudstam, L. G., Rusak, J. A., Salmaso, N., Samal, N. R., Schindler, D. E., Schladow, S. G., Schmid, M., Schmidt, S. R., Silow, E., Soylu, M. E., Teubner, K., Verburg, P., Voutilainen, A., Watkinson, A., Williamson, C. E., and Zhang, G.: Rapid and highly variable warming of lake surface waters around the globe, *Geophysical Research Letters*, 42, 10.1002/2015gl066235, 2015.

Obu, J., Westermann, S., Bartsch, A., Berdnikov, N., Christiansen, H. H., Dashtseren, A., Delaloye, R., Elberling, B., Etzelmüller, B., Kholodov, A., Khomutov, A., Kääb, A., Leibman, M. O., Lewkowicz, A. G., Panda, S. K., Romanovsky, V., Way, R. G., Westergaard-Nielsen, A., Wu, T., Yamkhin, J., and Zou, D.: Northern Hemisphere permafrost map based on TTOP modelling for 2000–2016 at 1 km² scale, *Earth Science Reviews*, 193, 299–316, 10.1016/j.earscirev.2019.04.023, 2019.

Oksanen, J., Simpson, G., Blanchet, F., Kindt, R., Legendre, P., Minchin, P., O'Hara, R., Solymos, P., Stevens, M., Szoecs, E., Wagner, H., Barbour, M., Bedward, M., Bolker, B., Borcard, D., Carvalho, G., Chirico, M., De Caceres, M., Durand, S., Evangelista, H., FitzJohn, R., Friendly, M., Furneaux, B., Hannigan, G., Hill, M., Lahti, L., McGlinn, D., Ouellette, M., Ribeiro Cunha, E., Smith, T., Stier, A., Ter Braak, C., and Weedon, J. Oksanen, J., Simpson, G. L., Blanchet, F. G., Kindt, R., Legendre, P., Minchin, P. R., et al.: Vegan: Community Ecology Package. R package version 2.6-4: <https://CRAN.R-project.org/package=vegan>, last access: 14. March 2024.

Opfergelt, S., Eirisdottir, E. S., Burton, K. W., Einarsson, A., Siebert, C., Gislason, S. R., and Halliday, A. N.: Quantifying the impact of freshwater diatom productivity on silicon isotopes and silicon fluxes: Lake Myvatn, Iceland, *Earth and Planetary Science Letters*, 305, 73–82, 10.1016/j.epsl.2011.02.043, 2011.

Pacyna, J. M., Travníkov, O., De Simone, F., Hedgecock, I. M., Sundseth, K., Pacyna, E. G., Steenhuisen, F., Pirrone, N., Munthe, J., and Kindbom, K.: Current and future levels of mercury atmospheric pollution on a global scale, *Atmos. Chem. Phys.*, 16, 12495–12511, 10.5194/acp-16-12495-2016, 2016.

Palagushkina, O., Nazarova, L., and Frolova, L.: Trends in development of diatom flora from sub-recent lake sediments of the Lake Bolshoy Kharbey (Bolshezemelskaya tundra, Russia), *Biological Communications*, 64, 244–251, 10.21638/spbu03.2019.403, 2020.

Palagushkina, O. V., Nazarova, L. B., Wetterich, S., and Schirrmeister, L.: Diatoms of modern bottom sediments in Siberian arctic, *Contemporary Problems of Ecology*, 5, 413–422, 10.1134/s1995425512040105, 2012.

Panizzo, V. N., Swann, G. E. A., Mackay, A. W., Vologina, E., Sturm, M., Pashley, V., and Horstwood, M. S. A.: Insights into the transfer of silicon isotopes into the sediment record, *Biogeosciences*, 13, 147–157, 10.5194/bg-13-147-2016, 2016.

Panizzo, V. N., Roberts, S., Swann, G. E. A., McGowan, S., Mackay, A. W., Vologina, E., Pashley, V., and Horstwood, M. S. A.: Spatial differences in dissolved silicon utilization in Lake Baikal, Siberia: Examining the impact of high diatom biomass events and eutrophication, *Limnology and Oceanography*, 63, 1562–1578, 10.1002/lno.10792, 2018.

Panizzo, V. N., Swann, G. E. A., Mackay, A. W., Vologina, E., Alleman, L., André, L., Pashley, V. H., and Horstwood, M. S. A.: Constraining modern-day silicon cycling in Lake Baikal, *Global Biogeochemical Cycles*, 31, 556–574, 10.1002/2016gb005518, 2017.

Paterson, A. M., Cumming, B. F., Smol, J. P., and Hall, R. I.: Marked recent increases of colonial scaled chrysophytes in boreal lakes: implications for the management of taste and odour events, *Freshwater Biology*, 49, 199–207, 10.1046/j.1365-2427.2003.01170.x, 2004.

Formatiert: Schriftfarbe: Akzent 6, Englisch (Vereinigtes Königreich)

Formatiert: Englisch (Vereinigtes Königreich)

Formatiert: Englisch (Vereinigtes Königreich)

Feldfunktion geändert

Formatiert: Englisch (Vereinigtes Königreich)

Formatiert: Schriftfarbe: Akzent 6, Englisch (Vereinigtes Königreich)

Formatiert: Englisch (Vereinigtes Königreich)

Formatiert: Englisch (Vereinigtes Königreich), Durchgestrichen

Formatiert: Englisch (Vereinigtes Königreich)

Formatiert: Schriftfarbe: Akzent 6, Englisch (Vereinigtes Königreich)

Formatiert: Englisch (Vereinigtes Königreich)

475 Pestryakova, L. A., Herzsuh, U., Gorodnichev, R., and Wetterich, S.: The sensitivity of diatom taxa
 from Yakutian lakes (north-eastern Siberia) to electrical conductivity and other environmental
 variables, *Polar Research*, 37, 1485625, 10.1080/17518369.2018.1485625, 2018.

480 Pestryakova, L. A., Herzsuh, U., Wetterich, S., and Ulrich, M.: Present-day variability and Holocene
 dynamics of permafrost-affected lakes in central Yakutia (Eastern Siberia) inferred from diatom
 records, *Quaternary Science Reviews*, 51, 56-70, 10.1016/j.quascirev.2012.06.020, 2012.

480 Philibert, A., Prairie, Y. T., Campbell, I., and Laird, L.: Effects of late Holocene wildfires on diatom
 assemblages in Christina Lake, Alberta, Canada, *Canadian Journal of Forest Research*, 33, 2405-2415,
 10.1139/x03-165, 2003.

485 R Core Team. R: A Language and Environment for Statistical Computing, R version 4.4.1:
<https://www.R-project.org/>, last access: 2024.

Reynolds, C. S., Huszar, V., Kruk, C., Naselli-Flores, L., and Melo, S.: Towards a functional classification
 of the freshwater phytoplankton, *J Plankton Res*, 24, 417-428, 10.1093/plankt/24.5.417, 2002.

Rimet, F., Druart, J. C., and Anneville, O.: Exploring the dynamics of plankton diatom communities in
 Lake Geneva using emergent self-organizing maps (1974-2007), *Ecological Informatics*, 4, 99-110,
 10.1016/j.ecoinf.2009.01.006, 2009.

490 Roberts, S., Adams, J. K., Mackay, A. W., Swann, G. E. A., McGowan, S., Rose, N. L., Panizzo, V., Yang,
 H., Vologina, E., Sturm, M., and Shchetnikov, A. A.: Mercury loading within the Selenga River basin and
 Lake Baikal, Siberia, *Environ Pollut*, 259, 113814, 10.1016/j.envpol.2019.113814, 2020.

495 Roberts, S. L., Swann, G. E. A., McGowan, S., Panizzo, V. N., Vologina, E. G., Sturm, M., and Mackay, A.
 W.: Diatom evidence of 20th century ecosystem change in Lake Baikal, Siberia, *PLoS One*, 13,
 e0208765, 10.1371/journal.pone.0208765, 2018.

Round, F. E., Crawford, R. M., and Mann, D. G.: *The diatoms: biology and morphology of the genera*,
 Cambridge University Press, 1990.

500 Rühland, K. and Smol, J. P.: Diatom shifts as evidence for recent Subarctic warming in a remote tundra
 lake, NWT, Canada, *Palaeogeography, Palaeoclimatology, Palaeoecology*, 226, 1-16,
 10.1016/j.palaeo.2005.05.001, 2005.

Rühland, K., Paterson, A. M., and Smol, J. P.: Hemispheric-scale patterns of climate-related shifts in
 planktonic diatoms from North American and European lakes, *Global Change Biology*, 14, 2740-2754,
 10.1111/j.1365-2486.2008.01670.x, 2008.

505 Rühland, K., Priesnitz, A., and Smol, J. P.: Paleolimnological Evidence from Diatoms for Recent
 Environmental Changes in 50 Lakes across Canadian Arctic Treeline, Arctic, Antarctic, and Alpine
 Research, 35, 110-123, 10.1657/1523-0430(2003)035[0110:Pefdrj]2.0.Co;2, 2003.

Rühland, K., Smol, J. P., Jasinski, J. P. P., and Warner, B. G.: Response of Diatoms and Other Siliceous
 Indicators to the Developmental History of a Peatland in the Tiksi Forest, Siberia, Russia, Arctic,
 Antarctic, and Alpine Research, 32, 167-178, 10.1080/15230430.2000.12003352, 2000.

510 Rühland, K. M., Paterson, A. M., and Smol, J. P.: Lake diatom responses to warming: reviewing the
 evidence, *Journal of Paleolimnology*, 54, 1-35, 10.1007/s10933-015-9837-3, 2015.

Rühland, K. M., Paterson, A. M., Keller, W., Michelutti, N., and Smol, J. P.: Global warming triggers the
 loss of a key Arctic refugium, *Proc Biol Sci*, 280, 20131887, 10.1098/rspb.2013.1887, 2013.

515 Rutkowski, C., Lenz, J., Lang, A., Wolter, J., Mothes, S., Reemtsma, T., Grosse, G., Ulrich, M., Fuchs, M.,
 Schirrmeister, L., Fedorov, A., Grigoriev, M., Lantuit, H., and Strauss, J.: Mercury in sediment core
 samples from deep Siberian ice-rich permafrost, *Frontiers in Earth Science*, 9, 718153,
 10.3389/feart.2021.718153, 2021.

520 Ryves, D. B., Juggins, S., Fritz, S. C., and Battarbee, R. W.: Experimental diatom dissolution and the
 quantification of microfossil preservation in sediments, *Palaeogeogr Palaeocl*, 172, 99-113,
 10.1016/S0031-0182(01)00273-5, 2001.

Saros, J. E. and Anderson, N. J.: The ecology of the planktonic diatom *Cyclotella* and its implications for
 global environmental change studies, *Biol Rev Camb Philos Soc*, 90, 522-541, 10.1111/brv.12120, 2015.

525 Saros, J. E., Michel, T. J., Interlandi, S. J., and Wolfe, A. P.: Resource requirements of *Asterionella*
formosa and *Fragilaria crotonensis* in oligotrophic alpine lakes: implications for recent phytoplankton

Formatiert: Englisch (Vereinigtes Königreich),
Durchgestrichen

Formatiert: Englisch (Vereinigtes Königreich)

Formatiert: Englisch (Vereinigtes Königreich),
Durchgestrichen

Formatiert: Englisch (Vereinigtes Königreich)

Feldfunktion geändert

Formatiert: Englisch (Vereinigtes Königreich)

Formatiert: Englisch (Vereinigtes Königreich)

Formatiert: Englisch (Vereinigtes Königreich),
Durchgestrichen

Formatiert: Schriftfarbe: Akzent 6, Englisch (Vereinigtes
Königreich)

Formatiert: Englisch (Vereinigtes Königreich)

Formatiert: Schriftfarbe: Akzent 6, Englisch (Vereinigtes
Königreich)

Formatiert: Englisch (Vereinigtes Königreich)

Formatiert: Englisch (Vereinigtes Königreich),
Durchgestrichen

Formatiert: Englisch (Vereinigtes Königreich)

Formatiert: Schriftfarbe: Akzent 6, Englisch (Vereinigtes
Königreich)

Formatiert: Englisch (Vereinigtes Königreich)

community reorganizations, Canadian Journal of Fisheries and Aquatic Sciences, 62, 1681-1689, 10.1139/f05-077, 2005.

Saros, J. E., Rose, K. C., Clow, D. W., Stephens, V. C., Nurse, A. B., Arnett, H. A., Stone, J. R., Williamson, C. E., and Wolfe, A. P.: Melting Alpine Glaciers Enrich High-Elevation Lakes with Reactive Nitrogen, Environmental Science & Technology, 44, 4891-4896, 10.1021/es100147j, 2010.

Saros, J. E., Stone, J. R., Pederson, G. T., Slemmons, K. E., Spanbauer, T., Schliep, A., Cahl, D., Williamson, C. E., and Engström, D. R.: Climate-induced changes in lake ecosystem structure inferred from coupled neo- and paleoecological approaches, Ecology, 93, 2155-2164, 10.1890/11-2218.1, 2012.

Schmidtbauer, K., Noble, P., Rosen, M., Conley, D. J., and Frings, P. J.: Linking silicon isotopic signatures with diatom communities, Geochim Cosmochim Acta, 323, 102-122, 10.1016/j.gca.2022.02.015, 2022.

Shestakova, A. A., Fedorov, A. N., Torgovkin, Y. I., Konstantinov, P. Y., Vasyliov, N. F., Kalinicheva, S. V., Samsonova, V. V., Hiyama, T., Iijima, Y., Park, H., Iwahana, G., and Gorokhov, A. N.: Mapping the Main Characteristics of Permafrost on the Basis of a Permafrost-Landscape Map of Yakutia Using GIS, Land, 10, 462, 10.3390/land10050462, 2021.

Sivarajah, B., Rühland, K. M., Labaj, A. L., Paterson, A. M., and Smol, J. P.: Why is the relative abundance of *Asterionella formosa* increasing in a Boreal Shield lake as nutrient levels decline?, Journal of Paleolimnology, 55, 357-367, 10.1007/s10933-016-9886-2, 2016.

Smol, J. P.: The Ratio of Diatom Frustules to Chrysophycean Statospores - a Useful Paleolimnological Index, Hydrobiologia, 123, 199-208, Doi 10.1007/Bf00034378, 1985.

Smol, J. P.: Lakes in the Anthropocene: Reflections on tracking ecosystem change in the Arctic, International Ecology Institute, Oldendorf/Luhe, Germany, 438 pp., <https://doi.org/10.1002/lob.10634>, 978-3-946729-30-3, 2023.

Smol, J. P. and Douglas, M. S. V.: From controversy to consensus: making the case for recent climate change in the Arctic using lake sediments, Frontiers in Ecology and the Environment, 5, 466-474, 10.1890/060162, 2007.

Smol, J. P. and Stoermer, E. F.: The diatoms: applications for the environmental and earth sciences, Cambridge University Press, Cambridge, New York, Melbourne, Madrid, Cape Town, Singapore, São Paulo, Dehli, Dubai, Tokyo, Mexico City, 687 pp., 9780521509961, 2010.

Smol, J. P., Charles, D., and Dr, W.: Mallomonadacean microfossil provide evidence of recent lake acidification, Nature, 307, 628-630, 1984.

Smol, J. P., Wolfe, A. P., Birks, H. J., Douglas, M. S., Jones, V. J., Korhola, A., Pienitz, R., Rühland, K., Sorvari, S., Antoniades, D., Brooks, S. J., Fallu, M. A., Hughes, M., Keatley, B. E., Laing, T. E., Michelutti, N., Nazarova, L., Nyman, M., Paterson, A. M., Perren, B., Quinlan, R., Rautio, M., Saulnier-Talbot, E., Siitonen, S., Solovieva, N., and Weckstrom, J.: Climate-driven regime shifts in the biological communities of arctic lakes, Proc Natl Acad Sci U S A, 102, 4397-4402, 10.1073/pnas.0500245102, 2005.

Sochuliakova, L., Sienkiewicz, E., Hamerlik, L., Svitok, M., Fidlerova, D., and Bitusik, P.: Reconstructing the Trophic History of an Alpine Lake (High Tatra Mts.) Using Subfossil Diatoms: Disentangling the Effects of Climate and Human Influence, Water Air Soil Pollut, 229, 289, 10.1007/s11270-018-3940-9, 2018.

Solovieva, N., Jones, V., Birks, J. H. B., Appleby, P., and Nazarova, L.: Diatom responses to 20th century climate warming in lakes from the northern Urals, Russia, Palaeogeography, Palaeoclimatology, Palaeoecology, 259, 96-106, 10.1016/j.palaeo.2007.10.001, 2008.

Sorvari, S., Korhola, A., and Thompson, R.: Lake diatom response to recent Arctic warming in Finnish Lapland, Global Change Biology, 8, 171-181, 10.1046/j.1365-2486.2002.00463.x, 2002.

Spaulding, S. A., Otu, M. K., Wolfe, A. P., and Baron, J. S.: Paleolimnological Records of Nitrogen Deposition in Shallow, High Elevation Lakes of Grand Teton National Park, Wyoming, U.S.A., Arctic, Antarctic, and Alpine Research, 47, 703-717, 10.1657/aaaar0015-008, 2018.

Spaulding, S. A., Potapova, M. G., Bishop, I. W., Lee, S. S., Gasperak, T. S., Jovanoska, E., Furey, P. C., and Edlund, M. B.: Diatoms.org: supporting taxonomists, connecting communities, Diatom Research, 36, 291-304, 10.1080/0269249X.2021.2006790, 2021.

Formatiert: Schriftfarbe: Akzent 6, Englisch (Vereinigtes Königreich)

Formatiert: Englisch (Vereinigtes Königreich)

Formatiert: Schriftfarbe: Akzent 6, Englisch (Vereinigtes Königreich)

Formatiert: Englisch (Vereinigtes Königreich), Durchgestrichen

Formatiert: Durchgestrichen

Formatiert: Englisch (Vereinigtes Königreich), Durchgestrichen

Formatiert: Englisch (Vereinigtes Königreich)

Formatiert: Englisch (Vereinigtes Königreich), Durchgestrichen

Formatiert: Englisch (Vereinigtes Königreich)

Formatiert: Englisch (Vereinigtes Königreich), Durchgestrichen

Formatiert: Englisch (Vereinigtes Königreich)

Steffen, W., Broadgate, W., Deutsch, L., Gaffney, O., and Ludwig, C.: The trajectory of the Anthropocene: The Great Acceleration, *The Anthropocene Review*, 2, 81-98, 10.1177/2053019614564785, 2015.

580 Stevenson, M. A., McGowan, S., Pearson, E. J., Swann, G. E. A., Leng, M. J., Jones, V. J., Bailey, J. J., Huang, X., and Whiteford, E.: Anthropocene climate warming enhances autochthonous carbon cycling in an upland Arctic lake, Disko Island, West Greenland, *Biogeosciences*, 18, 2465-2485, 10.5194/bg-18-2465-2021, 2021.

585 Stieg, A., Biskaborn, B. K., Herzschuh, U., Strauss, J., Lindemann, J., and Meyer, H.: Mercury from sediment short core EN18232-1 of Lake Khamra, SW Yakutia, Siberia, Russia. [dataset], <https://doi.org/10.1594/PANGAEA.962973>, 2024a.

Stieg, A., Biskaborn, B. K., Herzschuh, U., Strauss, J., Pestryakova, L., and Meyer, H.: Hydroclimatic anomalies detected by a sub-decadal diatom oxygen isotope record of the last 220 years from Lake Khamra, Siberia, *Clim. Past*, 20, 909-933, 10.5194/cp-20-909-2024, 2024b.

590 Streets, D. G., Devane, M. K., Lu, Z., Bond, T. C., Sunderland, E. M., and Jacob, D. J.: All-Time Releases of Mercury to the Atmosphere from Human Activities, *Environmental Science & Technology*, 45, 10485-10491, 10.1021/es202765m, 2011.

Sun, X., Mörtz, C.-M., Porcelli, D., Kutscher, L., Hirst, C., Murphy, M. J., Maximov, T., Petrov, R. E., Humborg, C., Schmitt, M., and Andersson, P. S.: Stable silicon isotopic compositions of the Lena River and its tributaries: Implications for silicon delivery to the Arctic Ocean, *Geochim Cosmochim Acta*, 241, 120-133, 10.1016/j.gca.2018.08.044, 2018.

595 Sundseth, K., Pacyna, J. M., Pacyna, E. G., Pirrone, N., and Thorne, R. J.: Global Sources and Pathways of Mercury in the Context of Human Health, *Int J Environ Res Public Health*, 14, 105, 10.3390/ijerph14010105, 2017.

600 Sutton, J. N., Varela, D. E., Brzezinski, M. A., and Beucher, C. P.: Species-dependent silicon isotope fractionation by marine diatoms, *Geochim Cosmochim Acta*, 104, 300-309, 10.1016/j.gca.2012.10.057, 2013.

Sutton, J. N., André, L., Cardinal, D., Conley, D. J., de Souza, G. F., Dean, J., Dodd, J., Ehlert, C., Ellwood, M. J., Frings, P. J., Grasse, P., Hendry, K., Leng, M. J., Michalopoulos, P., Panizzo, V. N., and Swann, G. E. A.: A Review of the Stable Isotope Bio-geochemistry of the Global Silicon Cycle and Its Associated Trace Elements, *Frontiers in Earth Science*, 5:112, 10.3389/feart.2017.00112, 2018.

605 Swann, G. E. A., Leng, M. J., Juschus, O., Melles, M., Brigham-Grette, J., and Sloane, H. J.: A combined oxygen and silicon diatom isotope record of Late Quaternary change in Lake El'gygytyn, North East Siberia, *Quaternary Science Reviews*, 29, 774-786, 10.1016/j.quascirev.2009.11.024, 2010.

610 Todd, M. C. and Mackay, A. W.: Large-scale climatic controls on Lake Baikal ice cover, *Journal of Climate*, 16, 3186-3199, Doi 10.1175/1520-0442(2003)016<3186:Lccolb>2.0.Co;2, 2003.

Varela, D. E., Pride, C. J., and Brzezinski, M. A.: Biological fractionation of silicon isotopes in Southern Ocean surface waters, *Global Biogeochemical Cycles*, 18, GB1047, 10.1029/2003gb002140, 2004.

615 Verburg, P.: The need to correct for the Suess effect in the application of $\delta^{13}\text{C}$ in sediment of autotrophic Lake Tanganyika, as a productivity proxy in the Anthropocene, *Journal of Paleolimnology*, 37, 591-602, 10.1007/s10933-006-9056-z, 2007.

Wang, L., Rioual, P., Panizzo, V. N., Lu, H., Gu, Z., Chu, G., Yang, D., Han, J., Liu, J., and Mackay, A. W.: A 1000-yr record of environmental change in NE China indicated by diatom assemblages from maar lake Erlongwan, *Quaternary Research*, 78, 24-34, 10.1016/j.yqres.2012.03.006, 2012.

620 Wang, Q., Kim, D., Dionysiou, D. D., Sorial, G. A., and Timberlake, D.: Sources and remediation for mercury contamination in aquatic systems—a literature review, *Environ Pollut*, 131, 323-336, 10.1016/j.envpol.2004.01.010, 2004.

Wei, T. and Simko, V.: R package 'corrplot': Visualization of a Correlation Matrix. (Version 0.92): <https://github.com/taiyun/corrplot>, last access: 25. February 2024.

625 Williams, M. W., Seibold, C., and Chowanski, K.: Storage and release of solutes from a subalpine seasonal snowpack: soil and stream water response, Niwot Ridge, Colorado, *Biogeochemistry*, 95, 77-94, 10.1007/s10533-009-9288-x, 2009.

Formatiert: Englisch (Vereinigtes Königreich)

Formatiert: Englisch (Vereinigtes Königreich)

Feldfunktion geändert

Formatiert: Schriftfarbe: Akzent 6, Englisch (Vereinigtes Königreich)

Formatiert: Englisch (Vereinigtes Königreich)

Formatiert: Schriftfarbe: Akzent 6, Englisch (Vereinigtes Königreich)

Formatiert: Englisch (Vereinigtes Königreich)

Formatiert: Schriftfarbe: Akzent 6, Englisch (Vereinigtes Königreich)

Formatiert: Englisch (Vereinigtes Königreich)

Formatiert: Englisch (Vereinigtes Königreich)

Formatiert: Englisch (Vereinigtes Königreich), Durchgestrichen

Formatiert: Schriftfarbe: Akzent 6, Englisch (Vereinigtes Königreich)

Formatiert: Englisch (Vereinigtes Königreich), Durchgestrichen

Formatiert: Durchgestrichen

Formatiert: Englisch (Vereinigtes Königreich), Durchgestrichen

Formatiert: Englisch (Vereinigtes Königreich)

630	<p>Winder, M. and Sommer, U.: Phytoplankton response to a changing climate, <i>Hydrobiologia</i>, 698, 5-16, 10.1007/s10750-012-1149-2, 2012.</p> <p>Wolfe, A. P., Hobbs, W. O., Birks, H. H., Briner, J. P., Holmgren, S. U., Ingólfsson, Ó., Kaushal, S. S., Miller, G. H., Pagani, M., Saros, J. E., and Vinebrooke, R. D.: Stratigraphic expressions of the Holocene–Anthropocene transition revealed in sediments from remote lakes, <i>Earth-Science Reviews</i>, 116, 17-34, 10.1016/j.earscirev.2012.11.001, 2013.</p>	<p>Formatiert: Schriftfarbe: Akzent 6, Englisch (Vereinigtes Königreich)</p>
635	<p>Wolfin, J. A. and Stone, J. R.: Diatoms as Indicators of Water level Change in Freshwater Lakes, in: <i>The Diatoms Applications to the Environmental and Earth Sciences</i>, edited by: Stoermer, E. F., and Smol, J. P., Cambridge University Press., 174–185, 2010.</p> <p>Woolway, R. I., Kraemer, B. M., Lenters, J. D., Merchant, C. J., O'Reilly, C. M., and Sharma, S.: Global lake responses to climate change, <i>Nature Reviews Earth & Environment</i>, 1, 388-403, 10.1038/s43017-020-0067-5, 2020.</p>	<p>Formatiert: Englisch (Vereinigtes Königreich), Durchgestrichen</p> <p>Formatiert: Schriftfarbe: Akzent 6, Englisch (Vereinigtes Königreich)</p>
640	<p>Yan, Y., Wang, L., Li, J., Li, J., Zou, Y., Zhang, J., Li, P., Liu, Y., Xu, B., Gu, Z., and Wan, X.: Diatom response to climatic warming over the last 200 years: A record from Gonghai Lake, North China, <i>Palaeogeography, Palaeoclimatology, Palaeoecology</i>, 495, 48–59, 10.1016/j.palaeo.2017.12.023, 2018.</p> <p>Zahajská, P., Olid, C., Stadmark, J., Fritz, S. C., Opfergelt, S., and Conley, D. J.: Modern silicon dynamics of a small high-latitude subarctic lake, <i>Biogeosciences</i>, 18, 2325-2345, 10.5194/bg-18-2325-2021, 2021a.</p>	<p>Formatiert: Englisch (Vereinigtes Königreich), Durchgestrichen</p> <p>Formatiert: Englisch (Vereinigtes Königreich)</p>
645	<p>Zahajská, P., Cartier, R., Fritz, S. C., Stadmark, J., Opfergelt, S., Yam, R., Shemesh, A., and Conley, D. J.: Impact of Holocene climate change on silicon cycling in Lake 850, Northern Sweden, <i>The Holocene</i>, 31, 1582-1592, 10.1177/09596836211025973, 2021b.</p>	<p>Formatiert: Englisch (Vereinigtes Königreich), Durchgestrichen</p>
650	<p>Zalasiewicz, J., Waters, C. N., Summerhayes, C. P., Wolfe, A. P., Barnosky, A. D., Cearreta, A., Crutzen, P., Ellis, E., Fairchild, I. J., Galuszka, A., Haff, P., Hajdas, I., Head, M. J., Ivar do Sul, J. A., Jeandel, C., Leinfelder, R., McNeill, J. R., Neal, C., Odada, E., Oreskes, N., Steffen, W., Syvitski, J., Vidas, D., Wapreisch, M., and Williams, M.: The Working Group on the Anthropocene: Summary of evidence and interim recommendations, <i>Anthropocene</i>, 19, 55–60, 10.1016/j.ancene.2017.09.001, 2017.</p>	<p>Formatiert: Englisch (Vereinigtes Königreich), Durchgestrichen</p>